KfK 4158
Oktober 1986

Investigations of Nuclear Projectile Break-up Reactions

A Laboratory Approach of Nuclear Astrophysics

H. Rebel
Institut für Kernphysik

Kernforschungszentrum Karlsruhe

KERNFORSCHUNGSZENTRUM KARLSRUHE

Institut für Kernphysik

KfK 4158

INVESTIGATIONS OF NUCLEAR PROJECTILE BREAK-UP REACTIONS

A LABORATORY APPROACH OF NUCLEAR ASTROPHYSICS

H. Rebel

Lectures presented at the International Summer School
"Symmetries and Semiclassical Features of Nuclear Dynamics"
1. - 13. September 1986, Poiana Brasov, Romania.

Kernforschungszentrum Karlsruhe GmbH, Karlsruhe

Kernforschungszentrum Karlsruhe GmbH
Postfach 3640, 7500 Karlsruhe 1

ISSN 0303-4003

ABSTRACT

The cross sections for radiative capture of α-particles, deuterons and protons by light nuclei at very low relative energies are of particular importance for the understanding of the nucleosynthesis of chemical elements and for determining the relative elemental abundances in stellar burning processes at various astrophysical sites. As example we quote the reactions $\alpha+d \rightarrow {}^{6}Li+\gamma$, $\alpha+{}^{3}He \rightarrow {}^{7}Be+\gamma$, or $\alpha+{}^{12}C \rightarrow {}^{16}O+\gamma$. As an alternative to the direct experimental study of these processes we consider the inverse process, the photodisintegration, by means of the virtual photons provided by a nuclear Coulomb field: $Z+a \rightarrow Z+b+c$. The radiative capture process $b+c \rightarrow a+\gamma$ is related to the inverse process, the photodisintegration $\gamma+a \rightarrow b+c$ by the detailed balance theorem. Except for the extreme case very close to the threshold the phase space favours the photodisintegration cross section as compared to the radiative capture.

The Coulomb dissociation cross section proves to be enhanced due to the large virtual photon number, seen by the passing projectile, and the kinematics of the process leads to particular advantages for studies of the interaction of the two break-up fragments at small relative energies E_{bc}. The conditions of dedicated experimental investigations are discussed and demonstrated by recent experimental and theoretical studies of the break-up of 156 MeV ${}^{6}Li$ projectiles. In addition, a brief review about general features of break-up processes of light ions in the field of atomic nuclei is given.

ZUSAMMENFASSUNG

Untersuchungen von Aufbruchreaktionen nuklearer Projektile - eine Labormethode der nuklearen Astrophysik

Die Wirkungsquerschnitte für den Strahlungseinfang von α-Teilchen, Deuteronen und Protonen an leichten Kernen bei sehr niedrigen Relativenergien sind von besonderer Bedeutung für das Verständnis der Nukleosynthese der chemischen Elemente und für die Bestimmung der Elementhäufigkeiten bei stellaren Brennprozessen. Als Beispiele betrachten wir die Reaktionen $\alpha+d \rightarrow {}^{6}Li+\gamma$, $\alpha+{}^{3}He \rightarrow {}^{7}Be+\gamma$ oder

$\alpha + {}^{12}C \rightarrow {}^{16}O + \gamma$. Als Alternative zu direkten Messungen dieser Prozesse betrachten wir den Umkehrprozess: die Photo-Dissoziation durch virtuelle Photonen des Coulombfeldes eines Kerns Z: $Z + a \rightarrow Z + b + c$. Dieser Prozess hängt über das Theorem des detaillierten Gleichgewichts mit dem Strahlungseinfang zusammen und ist vom Phasenraum in der Regel begünstigt.

Die Coulomb-Dissoziations-Wirkungsquerschnitte sind erhöht durch die große Zahl virtueller Photonen, die ein Projektil beim Durchflug des Coulombfeldes sieht. Die Kinematik des Aufbruchs führt zu besonderen Vorteilen für das Studium der Wechselwirkung der Aufbruchfragmente bei kleineren Relativenergien. Die Bedingungen gezielter experimenteller Untersuchungen werden diskutiert und dargelegt am Beispiel neuerer experimenteller und theoretischer Untersuchungen des Coulomb-Aufbruchs von 156 MeV ${}^{6}Li$-Projektilen. Darüber hinaus wird ein kurzer Überblick über generelle Phänomene des Aufbruchs leichter Ionen im Feld der Atomkerne gegeben.

CONTENT

1. INTRODUCTION

"Angesichts von Hindernissen
mag die kürzeste Linie zwischen zwei Punkten
die krumme sein"

Bertold Brecht, Leben des Galilei

There are many fields of scientific endevour in which nuclear physics plays a significant role but none appears to be more exciting in scope than astrophysics. All physical knowledge is clearly relevant in understanding our universe because of - in human scales - limitless ranges of temperature and density. Most objects in the universe are, of course, not accessible for an experimental analysis in our laboratories, and our fragmentary knowledge of these objects can be derived only indirectly through the study of various kinds of radiations and from the study of basic processes which are believed to contribute to the evolution of our universe.

Nuclear reactions are the source of energy for the vast majority of stars and, simultaneously, they produce the rich distribution of nuclides which we observe in our planetary system, in our galaxy, in solar and stellar atmospheres. Nuclear astrophysics is the endeavour to understand the birth of the chemical elements and of their isotopes. Guided by the actual knowledge about nuclear reaction cross sections and mechanisms, reaction networks of the nucleosynthesis in particular astrophysical situations are devised, like the familiar case of the pp chain - the way how our sun produces energy and converts hydrogen to helium (Fig. 1).

The pp chain is a combination of radiative capture reactions and weak interaction processes. The $^{3}He(^{4}He,\gamma)^{7}Be$ capture proceeds in a weak branch to ^{8}B which produces 75 % of the high-energy neutrinos, detected with Cl-detector in the Davis experiment.

In more massive stars, at higher temperature and density the hydrogen burning proceeds by the CNO cycle, provided one of the elements C, N or O is present as a catalyst (Fig. 1.2).

The original loop I, proposed by Bethe and Weizsäcker in 1938 is extended to a tri-cycle and can be closed by a $^{19}F(p,\alpha)$ reaction.

The "cold" cycle at a temperature of $T = 10^{7}K$ has the $^{14}N(p,\gamma)$ reaction as the slowest reaction, so that ^{12}C and ^{16}O are transformed in ^{14}N. This is different from the "warm" CNO cycle burning at $T = 1\text{-}2\cdot10^{8}K$, where the ß-decay of ^{13}N defines the speed of the reaction cycle.

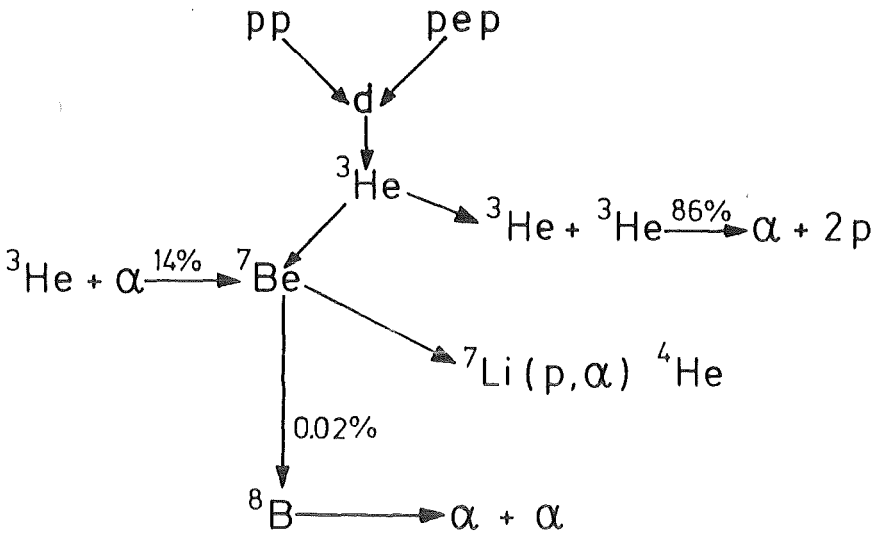

Fig.1.1 The proton-proton chain in the sun

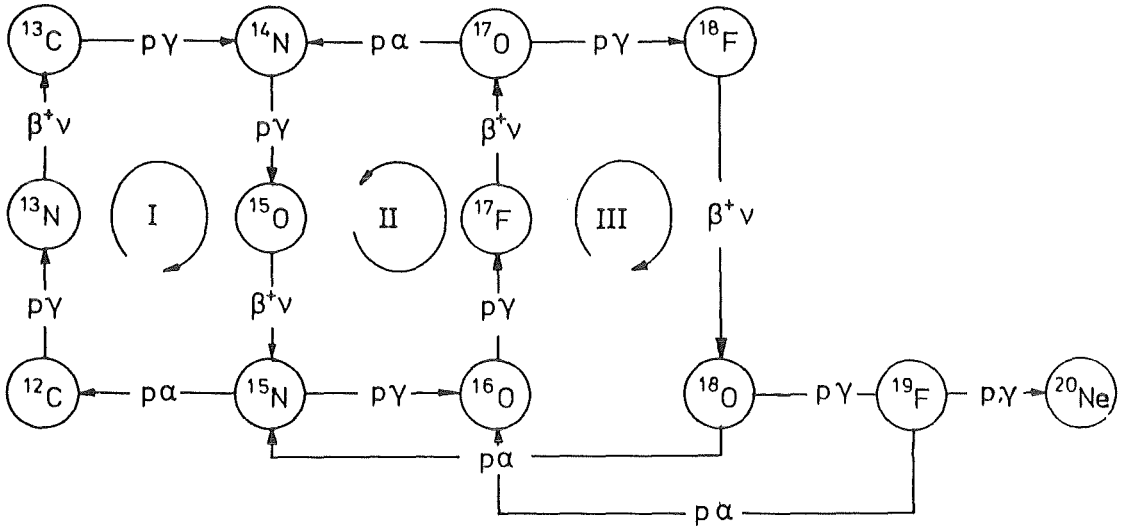

Fig. 1.2 CNO reaction cycles

There are astrophysical sites in very massive stars, in the convective shell of red giants, at explosive hydrogen-burning in nova and supernova-stars where reactions with radioactive nuclei compete with the ß-decay. The study of nuclear reactions with radioactive reaction partners, e.g. proton capture reactions of $^{13}N(T_{1/2} = 9.96m)$, $^{18}F(T_{1/2} = 110m)$ and many other reactions contributing to the nucleosynthesis at higher temperatures is a modern challenge for nuclear physics.

The essential parameters which govern the reaction net works are the Q-values and the stellare reaction rates. The rates are determined by the averaged reaction cross section

$$\langle\sigma v\rangle = \frac{(8/\pi)^{1/2}}{M^{1/2}(kT)^{3/2}} \int \sigma(E)\cdot E \exp(-E/kT)dE = f(T) \qquad (1.1)$$

i.e. the product of the energy-dependent cross section and the relative velocity of the interacting particles, averaged with the Maxwell-Boltzmann distribution at the temperature T. The calculation of $\langle\sigma v\rangle$ needs the knowledge of $\sigma(E)$ in the range of the so called Gamov-window i.e. the effective energy range of the nuclear burning, resulting from the interference of the Coulomb penetration and the Maxwell-Boltzmann distribution (Fig. 1.3).

Most of the laboratory approaches to experimental nuclear astrophysics, investigating charged-particle-induced reactions in stellar burning processes, involve the bombardment of rather thin targets by low-energy protons, ^3He, α-particles or other light ions. The cross sections are almost always needed at energies far below those for which measurements can be performed in the laboratory, and they must therefore be obtained by extrapolation from the laboratory energy region[1,2] using procedures which are not free from theoretical bias.

Tab. 1.1 presents some selected cases of interest at various astrophysical sites. The $^3He(^4He,\gamma)^7Be$ radiative capture reaction which at solar temperatures affects the solar neutrino flux and bears strongly on the longstanding solar neutrino problem[3,4], is experimentally studied[4,5] down to the CM-energy E_{CM}=165 keV, while the cross section is actually needed at 1-20 keV. A simi-

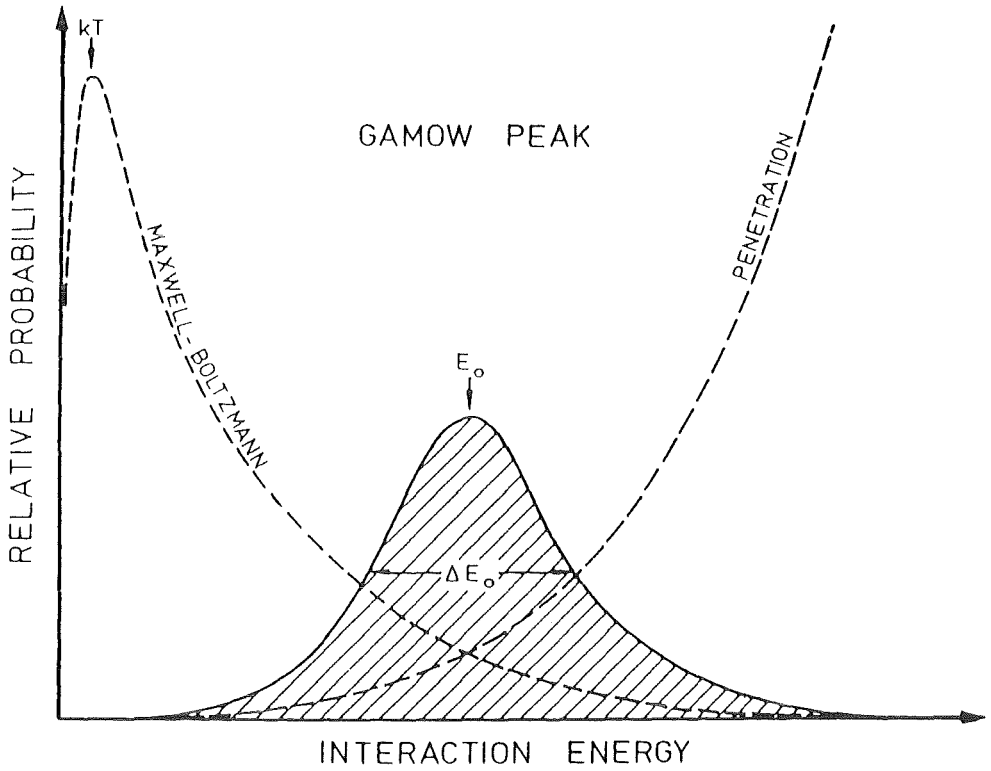

Fig. 1.3 Maxwell-Boltzmann distribution, Coulomb penetration factor and the effective energy range of stellar burning. The position and width of the Gamov peak vary with the temperature.

lar situation is found for the $^{12}C(\alpha,\gamma)^{16}O$ reaction[6] which is important for the stellar helium-burning processes in red giant stars. To which extent a nucleosynthesis of ^{7}Li and ^{6}Li takes place 100-500 sec after the beginning of the expansion of the universe is determined by the $(\alpha+t)$ and $(\alpha+d)$ radiative capture cross sections at a temperature near $10^{9}K$.[7,8] The capture reaction $D(\alpha,\gamma)^{6}Li$ has been studied in the laboratory at CM energies $E_{CM} \geq 1$ MeV[9], and the present statement that essentially all ^{6}Li is produced in the galactic cosmic rays rather than just after the primeval big bang is based on a purely theoret-

ical estimate and extrapolation of the reaction rate, whose uncertainty is not known[7]. On the other side the production of the Li-isotopes and the comparison with the actual abundances provide a stringent test of the assumptions of the standard big bang model (see also Ref. 10).

EXAMPLE	$E_{measured}$	ASTROPHYSICAL INTEREST
Hydrogen Burning $\alpha + {}^{3}He \rightarrow {}^{7}Be + \gamma$ $E_0 \approx 10$ keV	$\geqslant 165$ keV	Solar Neutrino Problem
Helium Burning $\alpha + {}^{12}C \rightarrow {}^{16}O + \gamma$ $E_0 \approx 300$ keV	$\geqslant 1.34$ MeV	Ashes of Red Giant (C/O Ratio)
Big Bang Nucleosynthesis $\alpha + t \rightarrow {}^{7}Li + \gamma$ $\alpha + d \rightarrow {}^{6}Li + \gamma$ $E_0 \approx 100$ keV	$\geqslant 1$ MeV	Li Be B Production Test of the Standard Big Bang Model

Tab. 1.1 Some examples of radiative nuclear capture reactions of actual astrophysical interest.

The direct capture process is a transition from a continuum state of the reaction partners, the relative motion of which is described by a Coulomb distorted wave, to a bound final state with a particular angular momentum, induced by the

electromagnetics interaction and with emission of γ-rays of corresponding multipolarities. This is schematically indicated in Fig. 1.4 for the example $^{16}O(p,\gamma)^{17}F$.

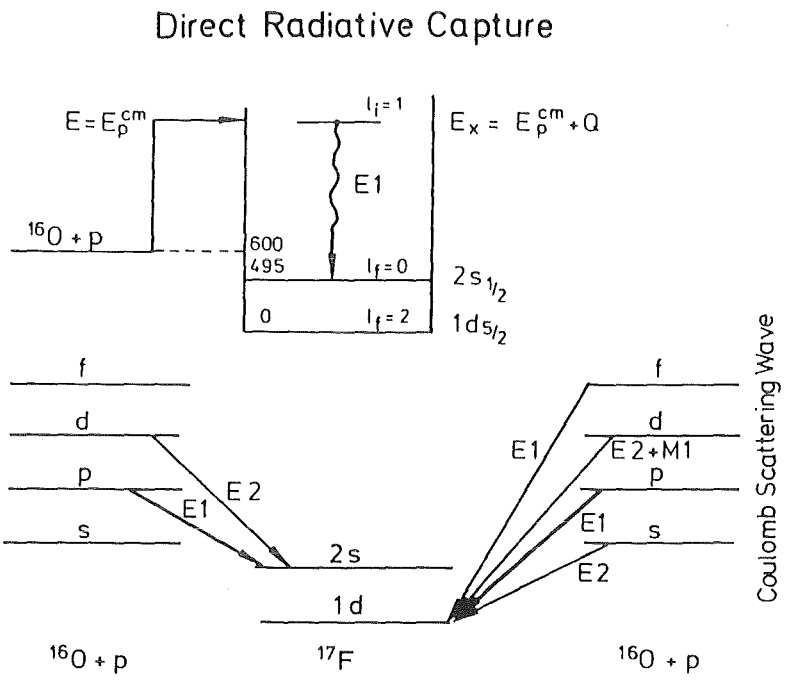

$$\sigma(E,LJ_i^{\pi}\rightarrow J_f^{\pi}) = \frac{e^2}{\hbar}\frac{8\pi(L+1)}{L[(2L+1)!!]^2}\, k_\gamma^{2L+1} B_{capt}(E,L,J_i^{\pi}-J_f^{\pi})$$

Fig. 1.4 Schematic scheme of direct capture transitions in the case of $^{16}O(p,\gamma)^{17}F$.

The capture cross section can be expressed in terms of an electromagnetic transition probability $B_{capt}(E,L)$ with the initial state being a (Coulomb) scattering state. Therefore B_{capt} is dependent from the energy in the entrance channel, dominated by the Coulomb barrier penetration which strongly suppresses the cross sections at small energies.

In cases of nonresonant direct capture reactions the energy dependence due to the Coulomb barrier penetration is usually factored out by a Gamov factor thus defining the astrophysical S-factor

$$S(E_{CM}) = \sigma_{capt} \cdot E_{CM} \exp(2\pi\eta) \qquad (1.2)$$

with the usual Coulomb parameter

$$\eta = \frac{Z_1 \cdot Z_2 \, e^2}{\hbar \, v}$$

in obvious notation. This S-factor shows a smooth energy dependence and seems to be adequate for an extrapolation to astrophysically relevant energy ranges. However, in most cases the extrapolation covers several orders of magnitude and is particularly suspect if resonances and subthreshold resonances are expected to be of influence.

In view of the considerable uncertainties of astrophysical considerations, introduced by the experimental difficulties in measuring radiative capture reactions, any alternative access to the reduced transition probabilities of the relevant transitions (between a bound state of the two nuclear particles and low-energy continuum states), is of interest.

In the present study we analyse a recently proposed[11-13] approach which suggests the use of the Coulomb field of a large Z nucleus for inducing photointegration processes of fast projectiles.

In fact, instead of studying directly the capture process

$$b + c \rightarrow a + \gamma \qquad (1.3)$$

one may consider the time reversed process (with a being in the groundstate)

$$\gamma + a \rightarrow b + c \qquad (1.4)$$

The corresponding cross sections are related by the detailed balance theorem

$$\sigma(b+c\rightarrow a+\gamma) = \frac{(2j_a+1)\,2}{(2j_b+1)\,(2j_c+1)} \; \frac{k_\gamma^2}{k^2} \; \sigma(a+\gamma\rightarrow b+c) \qquad (1.5)$$

The wave number in the (b+c) channel is

$$k^2 = \frac{2\mu_{bc} \, E_{CM}}{\hbar^2} \qquad (1.6)$$

with μ_{bc} the reduced mass while the photon wave number is given

$$k_\gamma = \frac{E_\gamma}{\hbar c} = \frac{E_{CM}+Q}{\hbar c} \qquad (1.7)$$

(neglecting a small recoil correction) in terms of the Q value of the capture reaction. Except for extreme cases very close to threshold ($k \to o$), the phase space favours the photodisintegration cross section as compared to the radiative capture. However, direct measurements of the photodisintegration near the break up threshold do hardly provide experimental advantages and seem presently impracticable (see Ref. 11). On the other hand the copious source of virtual photons acting on a fast charged nuclear projectile when passing the Coulomb field of a (large Z) nucleus offers a more promising way to study the photodisintegration process as Coulomb dissociation. Fig. 1.5 indicates schematically the dissociation reaction.

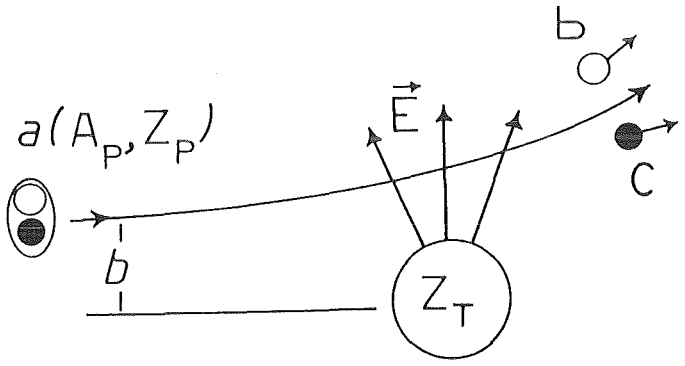

Fig. 1.5 Coulomb dissociation $a \to b + c$ in the field of a target nucleus (Z_T).

At a sufficiently high projectile energy the two fragments b and c emerge with rather high energies (around the beam-velocity energies) which facilitates the detection of these particles. At the same time the choice of adequate kinematical conditions for coincidence measurements allows to study rather low *relative* energies of b and c and to ensure that the target nucleus stays in the ground state (elastic break up). In addition, it turns out that the large number of virtual photons seen by the passing

projectile leads to an enhancement of the cross section, promising an experimental access to the electromagnetic transition matrix elements of interest.

Before illustrating this approach in more detail and considering the Coulomb break-up cross section for some actual cases, we review more general features and aspects of projectile break-up phenomena in nuclear reactions. The theoretical and experimental implications of the proposed Coulomb break-up investigations are discussed with reference to an actual example of current interest: the break-up of 156 MeV ^{6}Li projectiles.

2. GENERAL FEATURES OF BREAK-UP PROCESSES OF LIGHT IONS IN THE FIELD OF ATOMIC NUCLEI

"Wo da Ochsen sind, da ist der Stall unrein;
aber viel Gewinn ist durch die Stärke der Ochsen"

Bertold Brecht
Leben des Galilei (Sprüche Salomonis)

The break-up of composite nuclear projectiles in the field of a target nucleus is an important reaction mode of nucleus-nucleus collisions. This phenomenon is often signalled by broad and pronounced peaks in the continuum part of the inclusive spectra of the emitted particles. Fig. 2.1 - 2.2 display examples observed in nuclear reactions induced in collisions of 156 MeV ^{6}Li projectiles (which may decompose in various partitions (α+d), (^{3}He+t)...) with various target nuclei [14,15,16].

The most obvious characteristics of the bumps are the following:

(i) the bumps occur at beam-velocity energies. Deviations from this position near the grazing angle can be understood in terms of a deceleration of the projectile and an acceleration of the ejectile in the Coulomb-field of the target

(ii) the width of the bump is, in first order, proportional to $(E_{proj} \cdot \varepsilon)^{1/2}$ (ε being the binding energy of the projectile)

(iii) the cross section increases rapidly with decreasing emission angle

(iv) At forward angles the cross sections vary with the target mass with $A^{1/3} - A^{2/3}$

These features are consistent with a projectile break-up process.

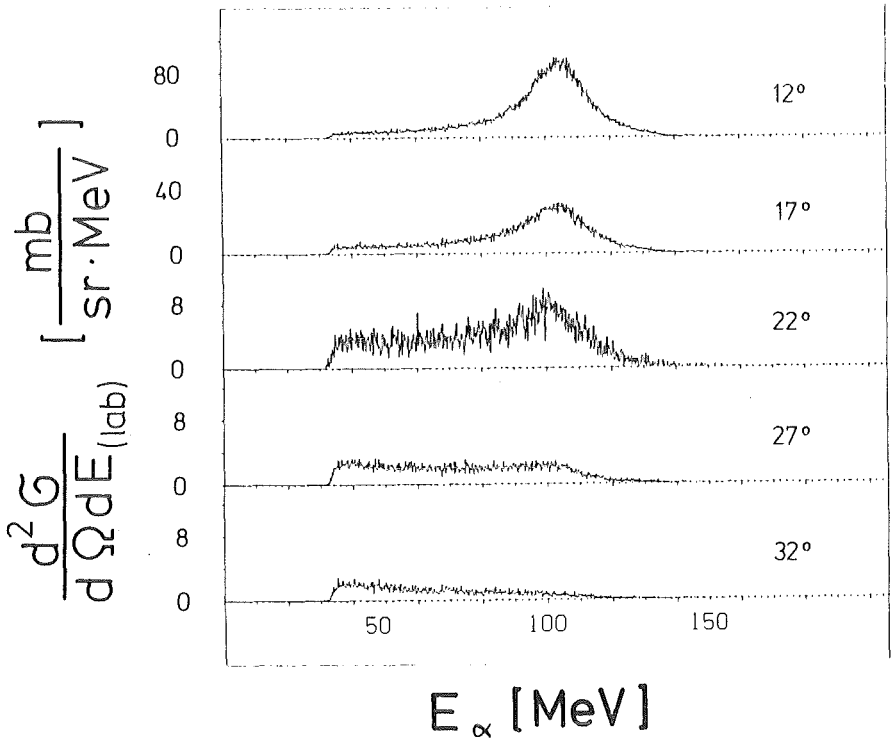

Fig. 2.1 Inclusive α-particle spectra from the ^{6}Li + ^{208}Pb reaction at E_{Li} = 156 MeV: ^{208}Pb + ^{6}Li → α + anything

Due to the pronounced cluster-structure of ^{6}Li the projectile break-up appears to be a rather prominent reaction mode, but fragmentation processes of both light and heavy ions interacting with nuclei comprise always a considerable fraction of the total reaction cross section at nonrelativistic and relativistic energies. Fig. 2.3 displays an example for fragmentation of ^{14}N at 60 MeV/amu, measured at GANIL (Ref. 16). The energy spectra of the emerging carbon isotopes show maxima at energy losses which correspond to the beam-velocity; the position and width of the "bumps" does not depend on the target mass, thus supporting a quasi-free process with minimum momentum change.

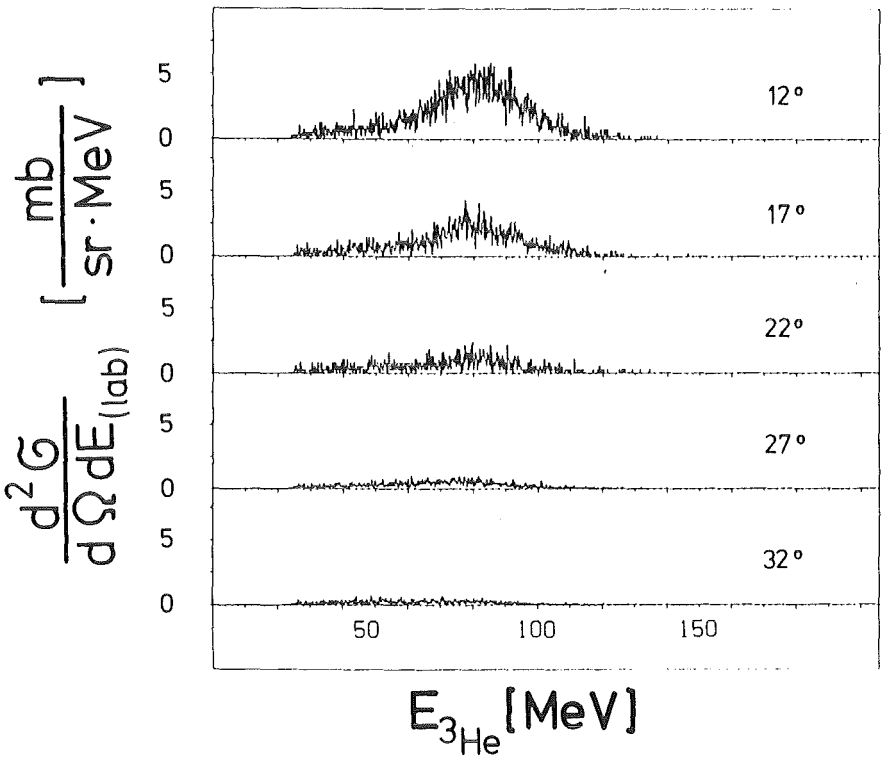

Fig. 2.2 Inclusive ^{3}He spectra from the ^{6}Li + ^{208}Pb reaction at E_{Li} = 156 MeV

A vast amount of experimental data of the break-up of deuterons, ^{3}He, ^{4}He (see Refs. 17,18), ^{6}Li (Refs. 19,14,15), ^{7}Li (Refs. 20-24) ^{9}Be(Ref. 25) and other heavier ions has been accumulated in inclusive and exclusive measurements for a wide range of incident beam energies. Even at rather low incident energies (< 10 MeV/amu) the break-up of carbon (Ref. 26), boron (Ref. 27), nitrogen (Ref. 28), oxygen (Refs. 28,30), fluorine (Ref. 31), and neon (Refs. 30,32) projectiles has been identified in the charged ejectile spectra.

The occurence of a bump at beam velocity energy with a strongly forward-peaked angular distribution suggests a fast process in which the observed particle remains practically undisturb-

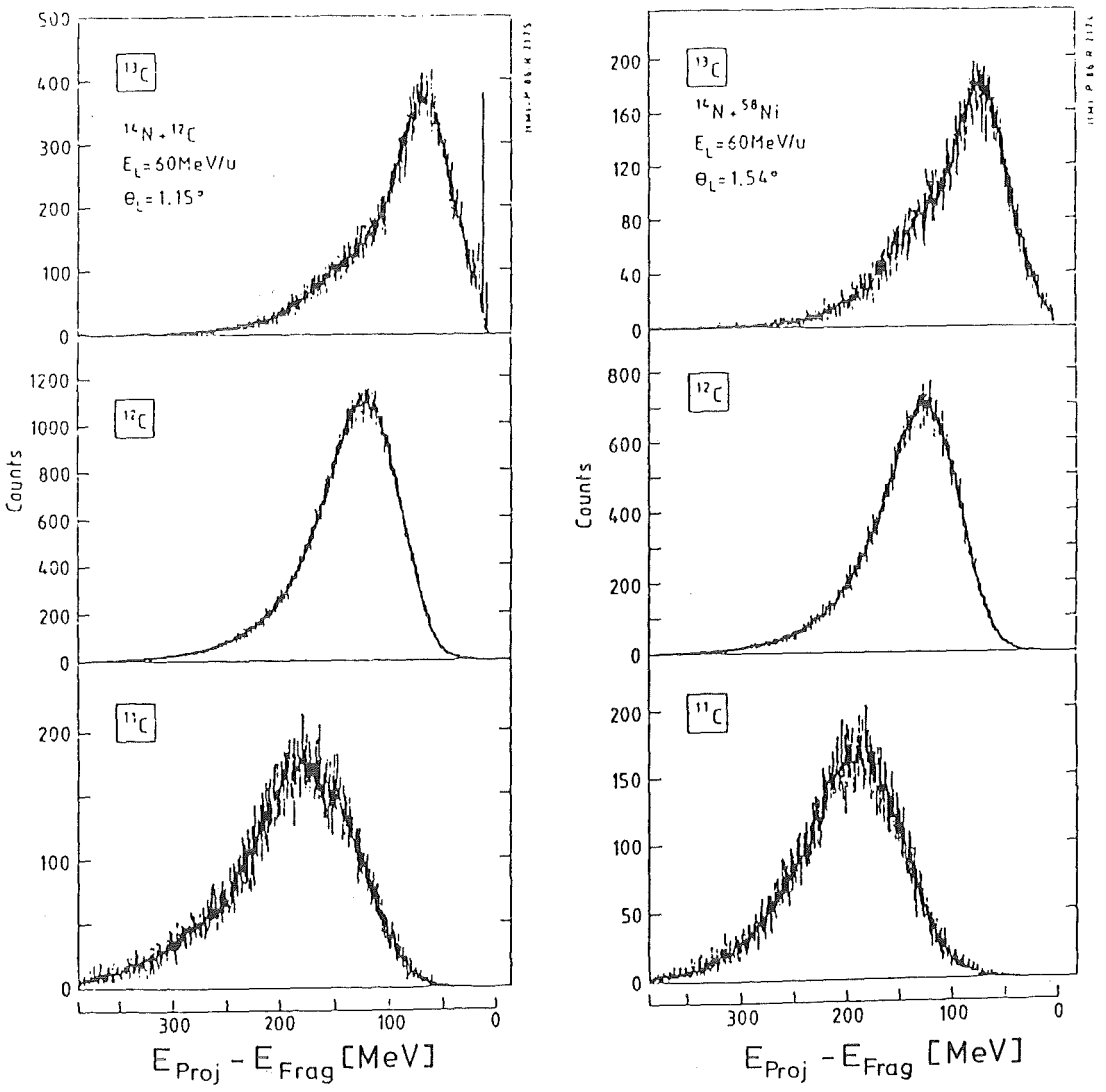

Fragmentation in ^{14}N induced reactions at 60 MeV/amu

Fig. 2.3 Spectra of the carbon isotopes from fragmentation of ^{14}N at 60 MeV/amu. The spectra show maxima at energy losses $E_{proj} - E_{frag}$ of $\Delta m \cdot 60$ MeV/amu

ed, being a spectator of the reaction. The basic mechanism is schematically displayed in Fig. 2.4. A projectile a = b + x with velocity $\vec{v}_a$ hits the nucleus A in a grazing collision and a spectator b moves on essentially undisturbed with its velocity before the collision i.e. the projectile velocity superimposed by the Fermi motion, while a participant x interacts strongly with target in variety of reaction modes (Fig. 2.5)

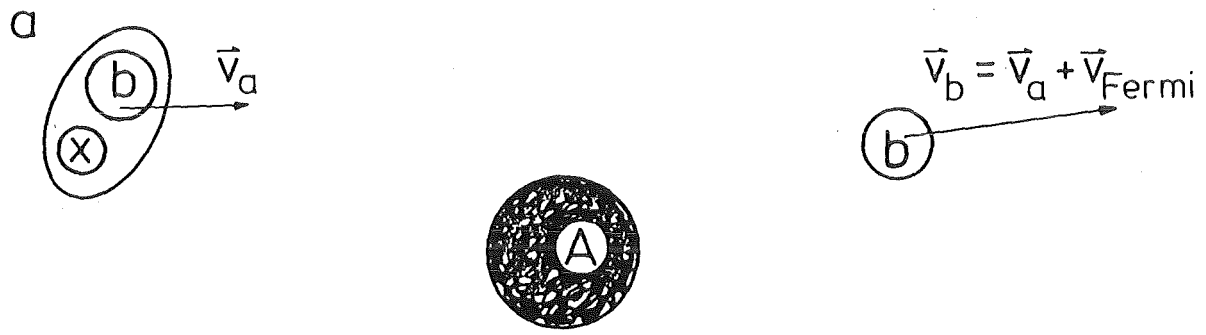

Fig. 2.4 Schematic picture of the break-up process

This main idea is already brought out by plane-wave descriptions [33,34] assuming a quasi-free break-up mechanism and relating the cross section to the squared Fourier transform of the projectile wave function, i.e. the intrinsic momentum distribution $|\phi(\vec{q})|^2$ of the nucleon-clusters in the projectile.

The laboratory momentum $\vec{p}_b$ of the considered fragment is given by a coupling of $\vec{q}$ and the momentum $\vec{p}_b^{\,o}$ due to the incident motion of the projectile. Assuming a Yukawa-type wave function

$$\psi(\vec{r}) = \sqrt{\frac{\alpha}{2\pi}} \frac{e^{-\alpha r}}{r} \qquad (2.1)$$

with $\alpha = \sqrt{2\mu\varepsilon}/h$ (μ = reduced mass and ε = separation energy), the double differential cross section is given by

$$\frac{d^2\sigma}{d\Omega_b dE_b} \propto m \cdot p |\psi(\vec{q})|^2 = mp \frac{\beta}{(\beta^2+q^2)^2} \qquad (2.2)$$

($\beta = \alpha \cdot h$) and

$$q^2 = p_b^2 + p_b^{o2} - 2p_b\, p_b^o \cos\theta_b$$

with θ_b being the emission angle of the fragment. Thus, for a fixed angle θ_b the shape of $d^2\sigma/d\Omega_b dE_b$ displays the distribution of the momentum q around $q_{min} = p_b^o \sin\theta_b$, or for a particular energy the variation of q with θ_b.

There is a modification of the Serber model with a completely opaque nucleus[33] which strips off the fragment, when striking the target, thus considerably reducing the quasifree cross section as calculated by assuming a transparent target nucleus. The opaque-nucleus version of the Serber model has been recently used for describing the break up of ^{7}Li at 11 MeV/nucleon[21]. The relative success of this model is shown in Fig. 2.6 presenting the inclusive α-particle spectrum observed for the emission angle $\theta = 9°$, when bombarding ^{40}Ca with 156 MeV ^{6}Li ions. The measured

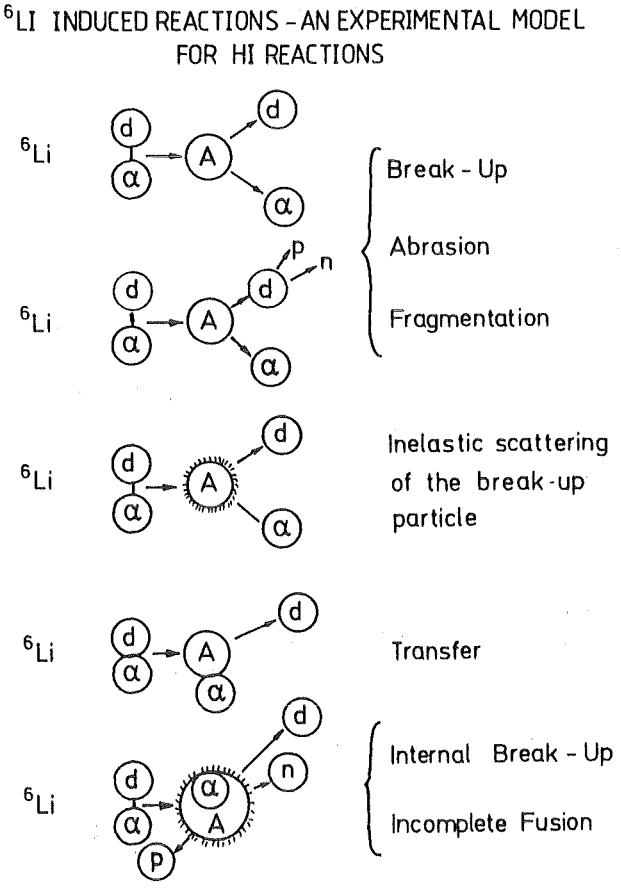

Fig. 2.5 Various reaction modes of ^{6}Li break-up

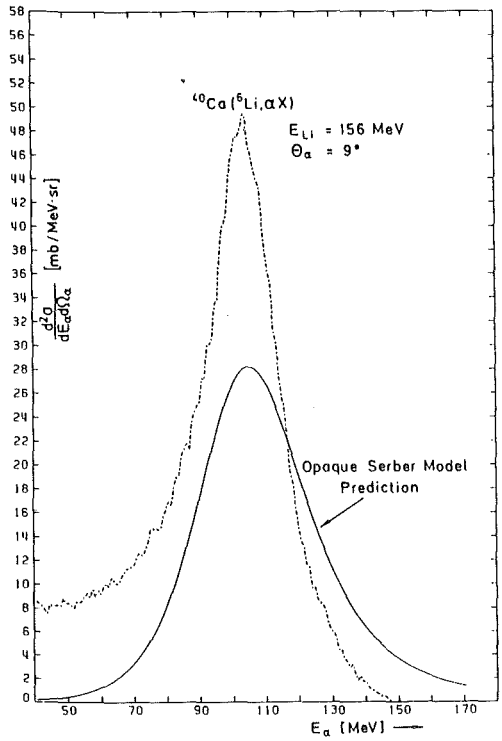

Fig. 2.6
Double differential cross section for inclusive emission of α-particles at 9° when bombarding ^{40}Ca by 156 MeV ^{6}Li ions. The theoretical curve is the prediction of the "Opaque-nucleus" Serber model[33] accounting for the nonelastic contribution.

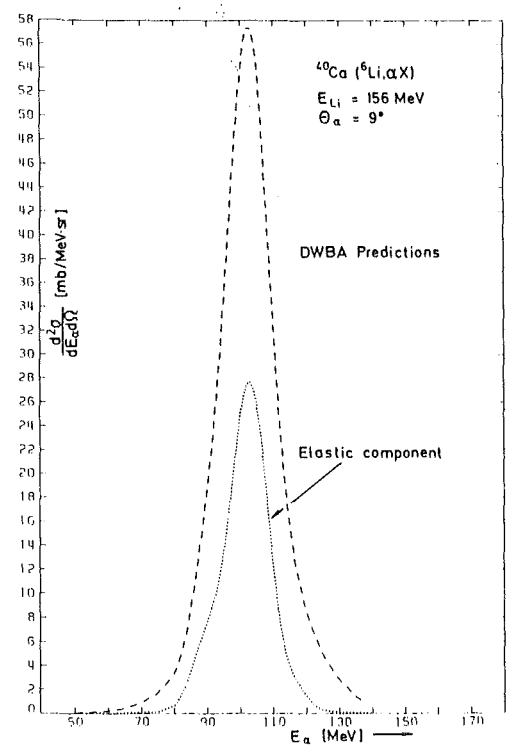

Fig. 2.7
DWBA prediction of the inclusive and elastic break-up for ^{40}Ca (^{6}Li,αx) at Θ_α = 9° and E_{Li} = 156 MeV.

cross section $d^2\sigma/d\Omega_\alpha dE_\alpha$ is compared with the calculated shape of the break-up fusion component, normalized in such a way that the $\tilde{\sigma}^{total}_{elast}/\sigma_{react}$ of the unobserved particle (deuteron) accounts globally for the contribution of elastic break-up. i.e. with elastic scattering of the deuteron by the *nuclear* potential.

Break up processes dominantly occur in a peripherial region of the nucleus where the nuclear potential is mainly responsible for elastic scattering. Ignoring the Coulomb potential in $\tilde{\sigma}^{total}_{elast}$ of the unobserved deuteron, the ratio $\tilde{\sigma}^{total}_{elast}/\sigma_{react}$ is the first guess for the ratio of elastic to nonelastic break-up.

The Serber model represents an immediate and direct break-up process of the projectile, in contrast to a two-step mechanism via inelastic excitation of the projectile to a resonance in the continuum (Fig. 2.8). The question whether the projectile break-up proceeds in a direct or a sequential way is often a matter of controversial discussion. It is known that the sequential break-up is dominating at energies near the Coulomb barrier, while for higher energies, especially for loosely bound particles, a direct break-up is expected to be of increased importance.

There are various advanced attempts[17,35,36] to describe the direct break-up process (see also Refs. 18,38). The most elaborate theory accounting for the absorption and distortion by the nuclear field is the post-form DWBA theory, worked out by Baur et al.[17] and successfully applied for analyses of experimental data in a variety of cases. In the present form the theory rests upon a zero-range approximation, which implies the internal momentum distribution of the cluster fragments being constrained to a Lorentzian shape (eq. 2.2) with parameters fixed by the binding energy ε. Fig. 2.7 displays an example for the ^{6}Li break-up with ^{40}Ca. The predicted elastic component (with ^{40}Ca remaining in the ground state) exhausts only 20 % of the inclusive cross section; consequently the supplement - the non-elastic component - should contribute with 80 %. This has been experimentally checked by exclusive studies measuring discrete γ-rays and charged particles emitted in coincidence [39].

The primary interest in studies of projectile break-up aims at a detailed understanding of the reaction mechanism and of the origin of various components observed and decomposed by specific exclusive studies. However, break-up reactions may be also considered as a tool for investigations of nuclear structure problems or as acess to "exotic" interactions of nuclear particles. In fact, since early studies[40] of nuclear reactions with more than two outgoing particles we know about the flexibility of such reactions

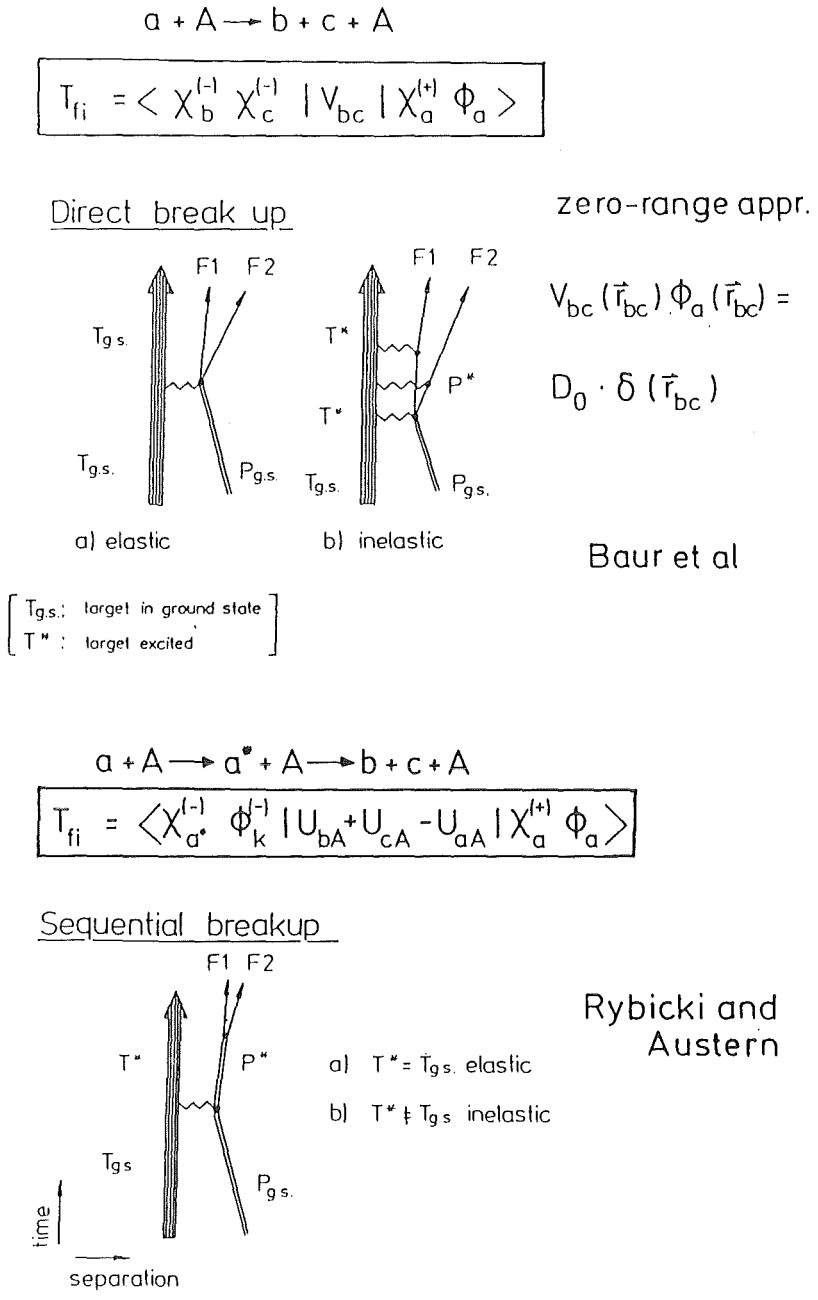

Fig. 2.8 Illustration of sequential and direct break-up processes with adequate DWBA amplitudes for the elastic mode.

and that they may provide useful information about the interaction in intermediate subsystems, otherwise hardly to study in pure two-body reactions. Recently, Baur[41] proposed the break-up of a composite projectile as a way to overcome the "trivial" hindrance by the Coulomb barrier in the incident channel of a low-energy charged particle induced reaction.

The principle is illustrated in Fig. 2.9 referring to the $^{18}O\ (p,\alpha)^{15}N$ reaction, which plays a role in the network of the CNO cycles (see Fig. 1.2). A "spectator" deuteron is attached to the proton to form a ^{3}He projectile. The bombarding energy E_{He} is large enough to overcome the Coulomb barrier, and the proton is brought into the nuclear reaction zone to induce the $p+^{18}O$ reaction. For astrophysical aspects, we are interested in cases when

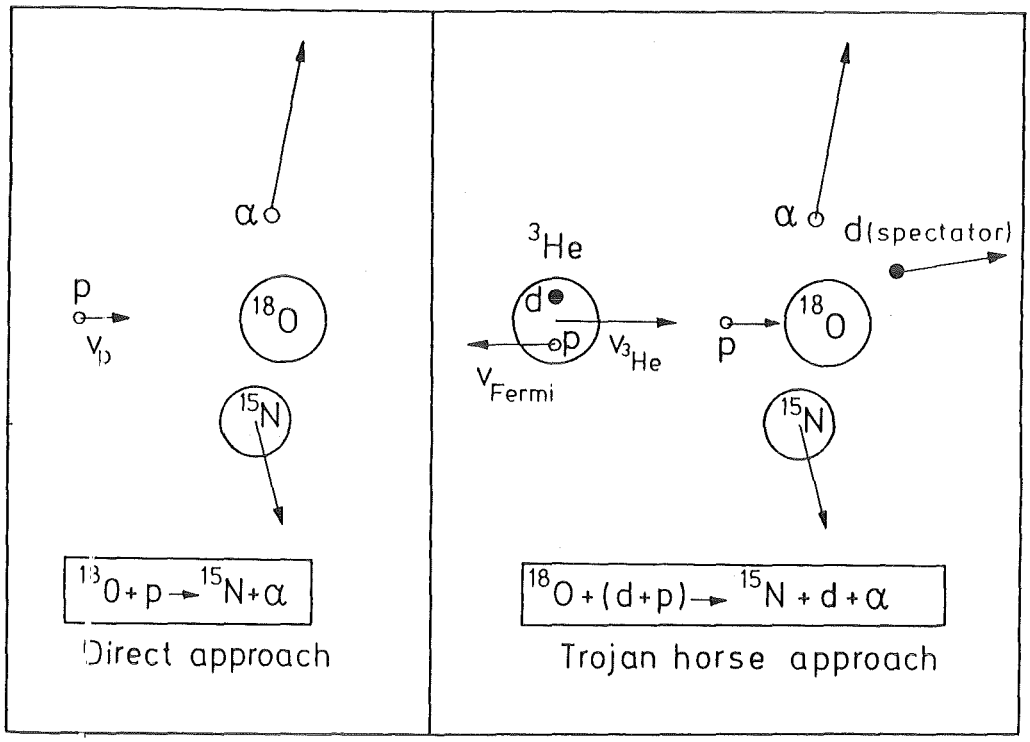

Fig. 2.9 The two-particle reaction is strongly hindered by the Coulomb barrier at astrophysically relevant energies. In the three-body approach ("Trojan horse") the interacting particle is brought into the interaction zone inside the projectile, and it induces the "low-energy reaction", if the Fermi motion nearly cancels the beam-velocity.

the Fermi motion of the proton inside the projectile nearly compensates the projectile velocity ("Tuning" of the relative energy by the Fermi motion). Of course, the interpretation of the coincidence cross section $d^3\sigma/d\Omega_\alpha d\Omega_d dE_d$ in terms of the two-body reaction of interest has to invoke a specific theory for the projectile break-up in the nuclear field (e.g. the DWBA theory, see Ref. 17), and the applicability of the proposed method is related to a detailed understanding of the *nuclear* reaction mechanism.

We have just mentioned this approach as an idea, and we pass to more details of the dissociation in the Coulomb field (Fig.1.5), which appears to be a more clean (though also indirect) access to inverse radiative capture reactions, as it is based on electromagnetic (photon exchange) interactions.

3. THE COULOMB BREAK-UP CROSS SECTION

"Mathematik ist eine kalte Hausgenossin, nicht?

Bertold Brecht, Leben des Galilei

The double-differential cross section for Coulomb excitation of a projectile by an electric multipole transition of the order L as given by the first order theory of Alder and Winther[42] can be rewritten in the form

$$\frac{d^2\sigma}{d\Omega dE_x} = \frac{1}{E_x} \frac{d\eta_{EL}}{d\Omega} \cdot \sigma_{EL}^{photo} \quad . \tag{3.1}$$

$$\sigma_{EL}^{photo} = \frac{(2\pi)^3(L+1)}{L[(2L+1!!]^2} k_\gamma^{2L-1} B(EL;I_i \to I_f) \rho_f(E_\gamma) \tag{3.2}$$

is related to the $B_{capt}(EL)$-value and the capture cross section, respectively. The function $d\eta_{EL}/d\Omega$ does not depend on the internal structure of the projectile. It only depends on the excitation energy E_γ and the relative motion. We call $d\eta_{EL}/d\Omega$ the *virtual photon number* per unit solid angle seen by the projectile, scattered by the Coulomb field. It actually depends on the incident

energy, the mass and Z of the projectile and of the impact parameter. This factorization of the cross section corresponds to the Weizsäcker-Williams method used for deriving the Coulomb dissociation cross section of relativistic projectiles. The virtual photon spectrum has been explored more in detail by several authors[43]. Fig. 3.1 displays the electric dipole component, relevant for the two considered examples: the dissociation of ^{7}Be and ^{16}O when passing ^{208}Pb with an impact parameter b = 10 fm at two different projectile energies. The corresponding break-up thresholds are marked.

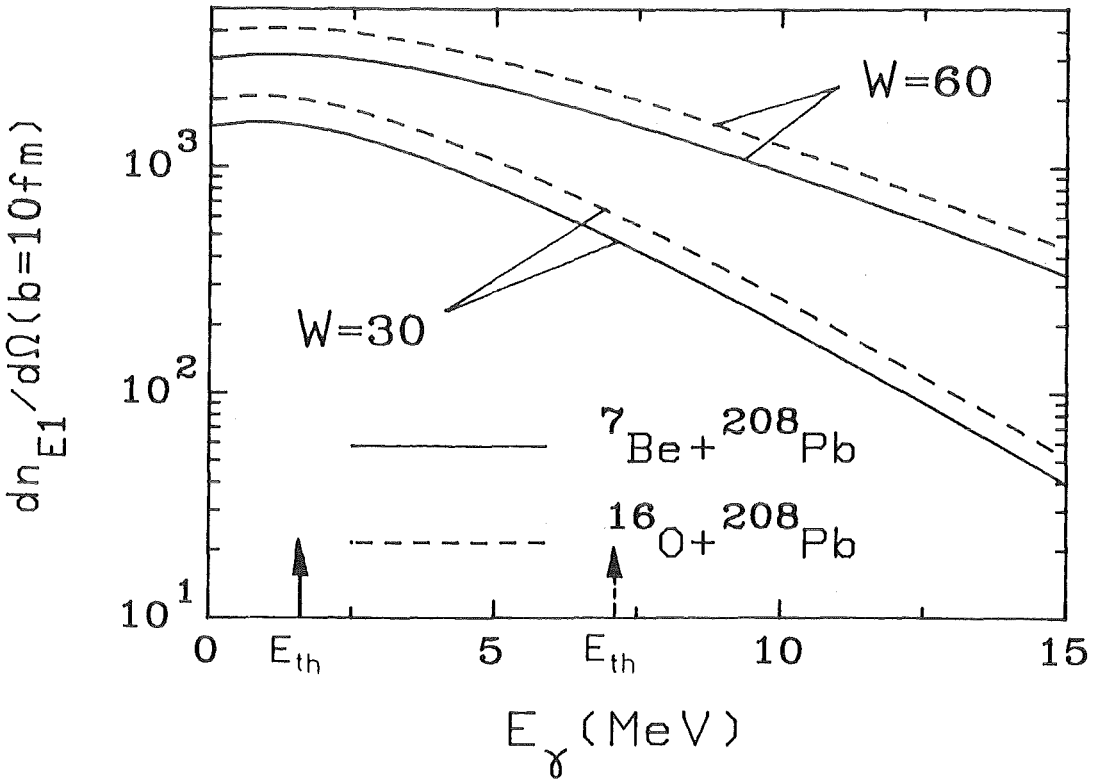

Fig. 3.1 E1 virtual photon spectra seen by the projectile with b = 10 fm at different projectile energies W (MeV/amu)

We are especially interested in the case where the scattering angle is small, $\Theta<<1$, i.e. $\varepsilon = \frac{1}{\sin\Theta/2} >> 1$. In this case we have

$$\frac{dn_{E1}}{d\Omega} = \frac{Z^2}{4\pi^2}\,\alpha\,\varepsilon^2\left(\frac{c}{v}\right)^2 x^2\{K_0^2(x)+K_1^2(x)\}^2 = \frac{Z^2}{4\pi^2}\,\alpha\,\varepsilon^2\left(\frac{c}{v}\right)^2\phi_1(x) \qquad (3.3)$$

where $x = \frac{\omega b}{v}$ is the adiabaticity parameter, v is the velocity of the projectile, $K_i(x)$ being the modified Bessel functions and $E_\gamma = h\omega$. Corrections due to Coulomb repulsion depend on $\xi = \frac{\omega a}{v}$, where a is half the distance of closest approach in a head on collision; they are small and easily evaluated. For the important E2 case we obtain

$$\frac{dn_{E2}}{d\Omega} = \frac{Z^2\alpha}{\pi^2} \frac{1}{\xi^2} \left(\frac{c}{v}\right)^4 \cdot \phi_2(x) \qquad (3.4)$$

where

$$\phi_2(x) = x^2\{K_1^2 + x^2(K_1^2+K_o^2) + xK_oK_1\} \qquad (3.5)$$

The functions ϕ_1 and ϕ_2 are given in Fig. 3.2.

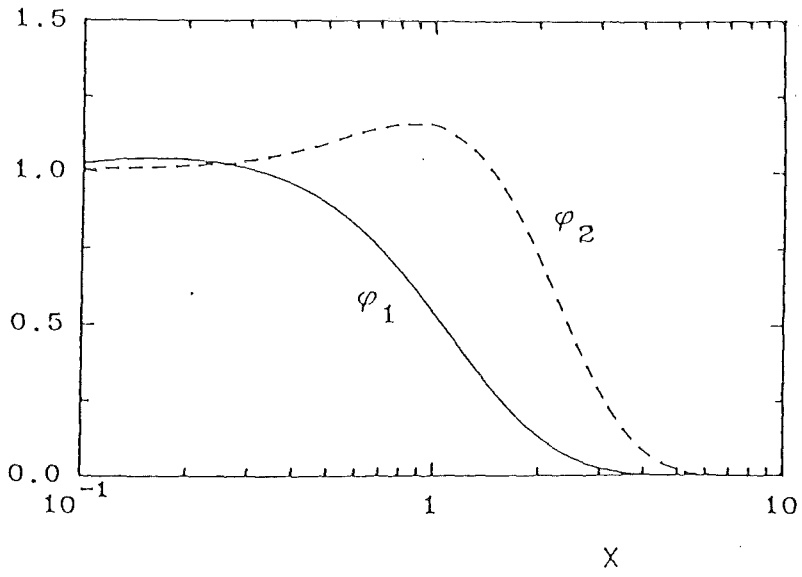

Fig. 3.2 The shape of the virtual photon spectrum as a function of the adiabaticity parameter x for the multipolarities E1 and E2.

It can be seen that the E2 virtual photon numbers are in many interesting cases much larger than the corresponding E1 ones. From various experimental conditions with different relative E1 and E2 virtual photon numbers the quantity $\sigma_{E\lambda}^{photo}$ can be individually determined. In coincidence studies interference effects between different multipoles will show up in general, which can in principle help to disentangle the various multipole contributions. A selective population of magnetic substates of the system b+c is expected. It can be directly calculated from the theory of Coulomb excitation.

The most interesting feature is the high intensity of the virtual photon spectra which actually leads to an enormous enhancement of the photodissociation cross section. This is one of the main advantages of the proposed method. The examples given in Tab. 3.1 demonstrate the effect. The table gives the double-differential cross sections for the excitation of the projectile to the continuum energy E_{bc} of the emerging fragments when the projectile or the fragment center-of-mass, respectively, is scattered to $d\Omega$. Assuming a specific detection geometry, this cross section can be transformed* into the triple differential cross section, which we are actually going to measure. Obviously the resulting values appear to be experimentally accessible, in contrast to the corresponding σ_{capt}-values.

REACTION b + c ↔ a	E_{bc} [MeV]	σ_{capt} [n b]	$\frac{d^2\sigma^{Diss}}{dE_{bc}\, d\Omega}$ [μb MeV^{-1} sterad^{-1}]	$\frac{d^3\sigma^{Diss}}{dE_b\, d\Omega_b\, d\Omega_c}$ [μb MeV^{-1} sterad^{-2}]	E_{thr} [MeV]
E1 $\alpha + {}^3He \leftrightarrow {}^7Be$	0.1	≈ 0.5	11	52 $\theta_\alpha = 5°$, $\theta_{He} = 7°$	1.58
E1 $\alpha + {}^{12}C \leftrightarrow {}^{16}O$	1.0	≈ 0.1	2		7.162
E2 $\alpha + d \leftrightarrow {}^6Li$	0.5	≈ 1.0	10^4		1.47
			Elastic Coulomb break up with ^{208}Pb E_{Proj} = 30 MeV/ amu - Impact parameter 10 fm		

Tab. 3.1 Numerical values of break-up cross sections for selected examples of astrophysical interest.

As the quadrupole component of the virtual photon field is much stronger than the E1 component at the particular values of the impact parameter and projectile energy, the ^6Li break-up is enhanced. For large b the E1 component would dominate. A more detailed account of the theoretical basis and calculations of the Coulomb break-up cross section is given in Ref. 13.

---

* For sake of simplicity isotropic decay of the excited projectile has been assumed for the example given in Tab. 3.1.

4. BASIC KINEMATICS OF EXCLUSIVE EXPERIMENTAL STUDIES

"Es ist ihr Ziel..... eine Grenze zu setzen
dem unendlichen Irrtum"

Bertold Brecht, Leben des Galilei

In a kinematically complete experiment, studying nuclear reactions with three outgoing particles

$$a + A \rightarrow b + c + A' \tag{4.1}$$

two particles are detected in coincidence at angles (Θ_b, ϕ_b) and (Θ_c, ϕ_c) with laboratory energies E_b and E_c, which are related to each other, if an additional condition is imposed. Such an condition can be the total reaction Q_3-value, which is composed of the three-body ground-state Q-value

$$Q_3^{ggg} = m_a + m_A - m_b - m_c - m_{A'} \tag{4.2}$$

and of the excitation energies of the ejectiles

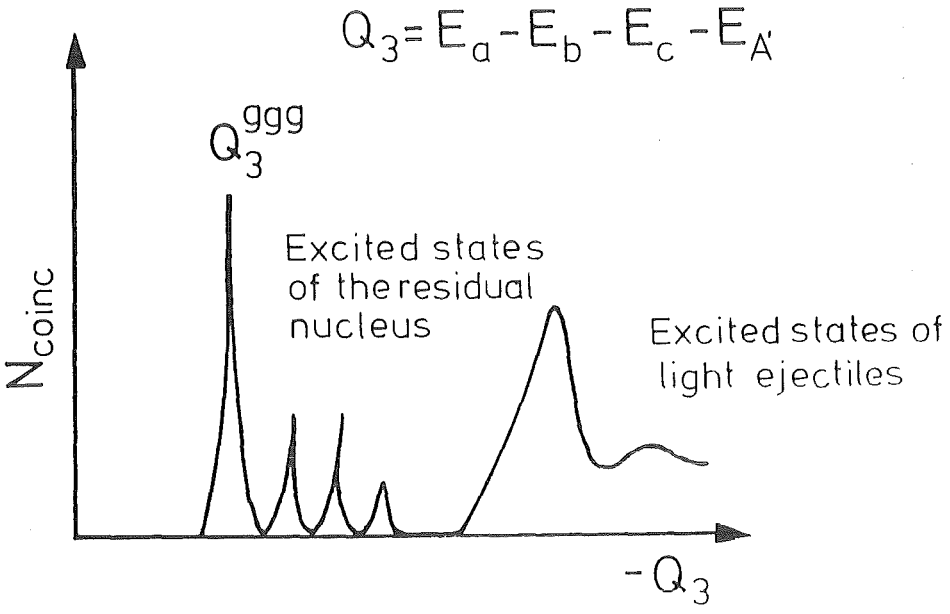

Fig. 4.1 Various components of the Q_3 spectrum

Q_3^{ggg} is just the break-up threshold Q_{th} in projectile break-up reactions. For a fixed Q_3-value the nonrelativistic relation between E_b and E_c is given by

$$E_b(m_b+m_c) + E_c(m_c+m_{A'}) - 2\sqrt{m_a m_b E_a E_b}\ \cos\Theta_b$$

$$- 2\sqrt{m_a m_c E_a E_c}\ \cos\Theta_c + 2\sqrt{m_b m_c E_b E_c}\ \cos\Theta_{bc} =$$

$$m_{A'} \cdot Q_3 + E_a\ (m_{A'}-m_a) \qquad (4.3)$$

Here is

$$\cos\Theta_{bc} = \cos\Theta_b\ \cos\Theta_c - \sin\Theta_b\ \sin\Theta_c\ \cos(\phi_b-\phi_c) \qquad (4.4)$$

In Fig. 4.2 the kinematic loci for the elastic break-up reaction

$$^6Li + {}^{208}Pb \rightarrow \alpha+d + {}^{208}Pb_{g.s.}$$

at E_{Li} = 156 MeV ($Q_3 = Q_3^{ggg} = Q_{th}$ = -1.47 MeV) is displayed by a E_d v.s. E_α spectrum. For $m_{b,c} << m_{A'}$ and at incident energies $>> Q_3$ the kinematic loci are single-valued and almost straight lines, since the recoil energy of ^{208}Pb is almost independent from E_b and E_c.

In general eq. 4.3 describes closed (double valued) curves in the E_b-E_c-plane. For a fixed Q-value and fixed energy E_b the two values of E_c correspond to cases where the (unobserved) recoiling nucleus (A') is emitted at a forward or a backward angle, respectively.

The projection of the cross section along the kinematical locus, say on the E_b axis $d^3\sigma/d\Omega_b d\Omega_c dE_b$ is a usual representation (in general by two branches) of the results.

A quantity of considerable interest is the *relative* kinetic energy in the rest frame of two ejectiles (say b and c)

$$E_{bc} = \frac{1}{m_b+m_c}\ [m_c E_b + m_b E_c - 2\sqrt{m_b m_c E_b E_c}\ \cos\Theta_{bc}] \qquad (4.5)$$

If the reaction proceeds in a two-step process via an intermediate excited system $(bc)^*$,

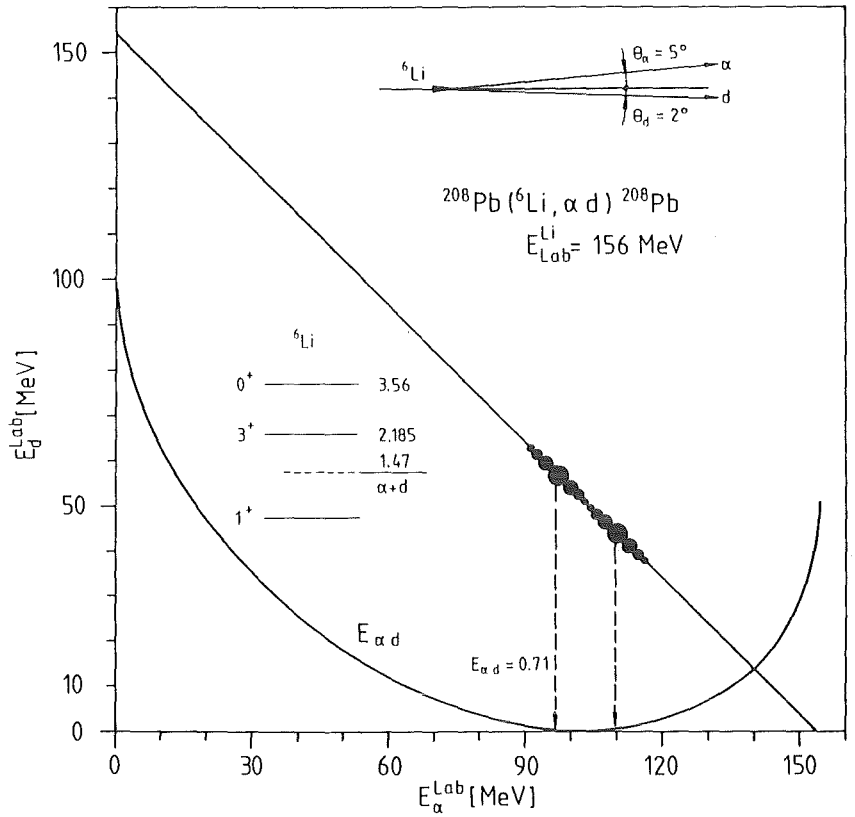

Fig. 4.2 Kinematic loci of the emerging deuteron and α-particles from elastic ^{6}Li break-up on ^{208}Pb at E_{lab} = 26 MeV/amu

$$E_{bc} = E^*(bc) + Q_{th} \qquad (4.6)$$

is the difference between the excitation energy $E^*(bc)$ of the decaying system and the decay threshold. In the case that the two-particle cross section of, e.g. particles b and c exhibits a narrow resonance at a certain relative energy, a peak of the three-particle cross-section is intuitively expected.

Fig. 4.2 shows additionally the relative energy $E_{\alpha d}$ plotted over the E_α^{Lab} axis for the ^{6}Li + ^{208}Pb → α+d + ^{208}Pb$_{g.s.}$ case. One recognizes that a particular $E_{\alpha d}$ value appears twice (once the α-particle being the slower fragment, once the deuteron). The minimum value of E_{bc} depends on the relative angle Θ_{bc} (Fig. 4.3). There is a remarkably slow variation of E_{bc} around the

minimum value ("magnifying glass effect") which leads to a good energy resolution on the relative energy scale.

Usually E_{bc} is the difference between two large quantities (see eq. 4.5), and due to considerable cancellations of various contributions, the energy resolution dE_{bc} is much better than on the scale of the laboratory energies E_b and E_c.

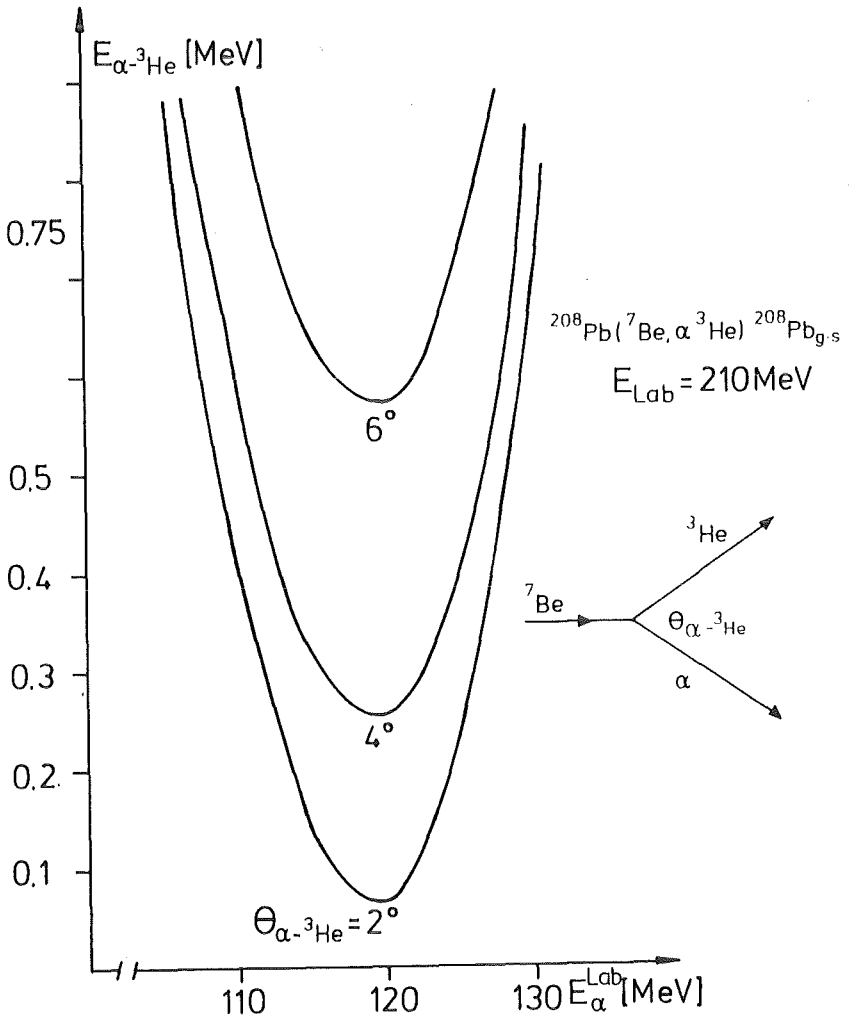

Fig. 4.3 Variation of the minimum value of the relative kinetic energy of the break-up fragments with their relative emission angle in the case of the ^{208}Pb $(^7Be, \alpha\,^3He)\,^{208}Pb_{g.s.}$ reaction at E_{Be} = 210 MeV.

Since for the velocities v_{bc}, v_b, v_c

$$v_{bc}^2 = v_b^2 + v_c^2 - 2\, v_b v_c \cos\theta_{bc} \qquad (4.7)$$

it is

$$v_{bc}dv_{bc} = (v_b - v_c \cos\theta_{bc})dv_b + (v_c - v_b \cos\theta_{bc})dv_c \qquad (4.8)$$

For beam-velocity particles ($v_b \approx v_c$) emerging within a narrow angle cone ($\cos\theta_{bc} \approx 1$), it is obvious

$$dE_{bc} < dE_b,\ dE_c$$

However, the determination of E_{bc} is especially sensitive to the spread in θ_{bc}

$$dE_{bc} = \frac{2\sqrt{m_b \cdot m_c \cdot E_b \cdot E_c}}{m_b + m_c} \sin\theta_{bc}\, d\theta_{bc} \qquad (4.9)$$

This sensititvity requires a good angular accuracy of the experimental set-up, and the choice of small θ_{bc}-values is favourable.

The analysis of the experimental results requires the representation of the laboratory cross sections in appropriate CM systems. In the case that the reaction proceeds via an intermediate system $(bc)^*$ (sequential decay), we have to consider the system A' - (bc) for the reaction $a+A \rightarrow A'+(bc)^*$, and the system b-c for the decaying "particle" $(bc)^*$. The transformation

$$\frac{d^3\sigma}{d\Omega_{A'-(bc)}\, d\Omega_{b-c}\, dE_{bc}} = J^{-1}\, \frac{d^3\sigma}{d\Omega_b d\Omega_c\, dE_b}$$

and involved Jacobians are worked out by Ohlsen[44] and Fuchs[45]. Fig. 4.3 indicates the relation of the various CM systems and the laboratory system.

An example for the transformation is given in Tab. 3.1 (with the notation $d\Omega_{b-c} \equiv d\Omega$). The simplification of an isotropic decay is not necessary, as the angular distribution can be theoretically calculated.

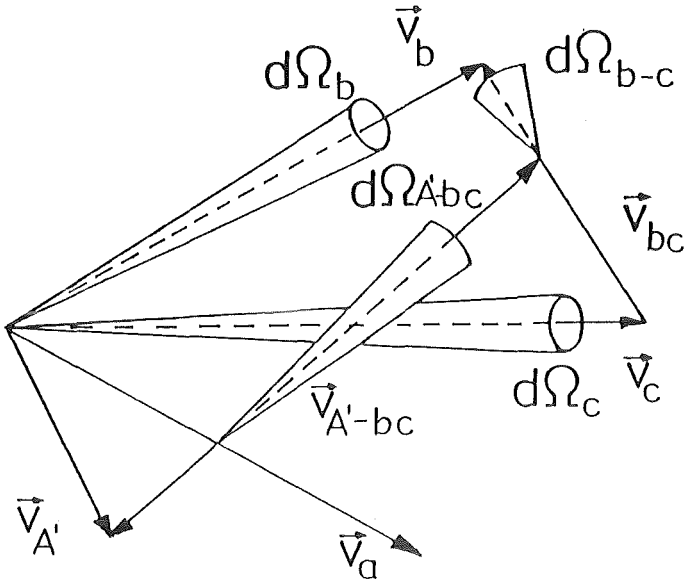

Fig. 4.4 Relation between the laboratory system ($\vec{v}_b, d\Omega_b, \vec{v}_c, d\Omega_c$) and the CM systems (b-c) and (A'-(bc)). The quantity v_{bc} describes the relative motion of particle b with respect to particle c, while $d\Omega_{b-c}$ denotes the solid angle of particle b from the CM of the (b-c) system.

5. COULOMB BREAK-UP OF ^{6}Li

"Unsere Unwissenheit ist unendlich,
tragen wir einen Kubikmillimeter ab!"

Bertold Brecht, Leben des Galilei

The light chemical elements with A<12 are not stellar ashes as they are too fragile at temperatures and densities as encountered in the stellar interior. They are rapidly "burned" away and transformed by proton induced reactions, in particular by (p,α) processes. Their origin is believed to be spallation reactions of the more abundant cosmic ray nuclides (^{12}C, ^{14}N, ^{16}O) with the interstellar medium[46], and in addition an explosive nucleosynthesis accompanying the early expansion of the universe from an initial hot dense singularity, the primordial "fire-ball" (big bang).[7,8,47]

BIG-BANG NUCLEOSYNTHESIS REVISITED

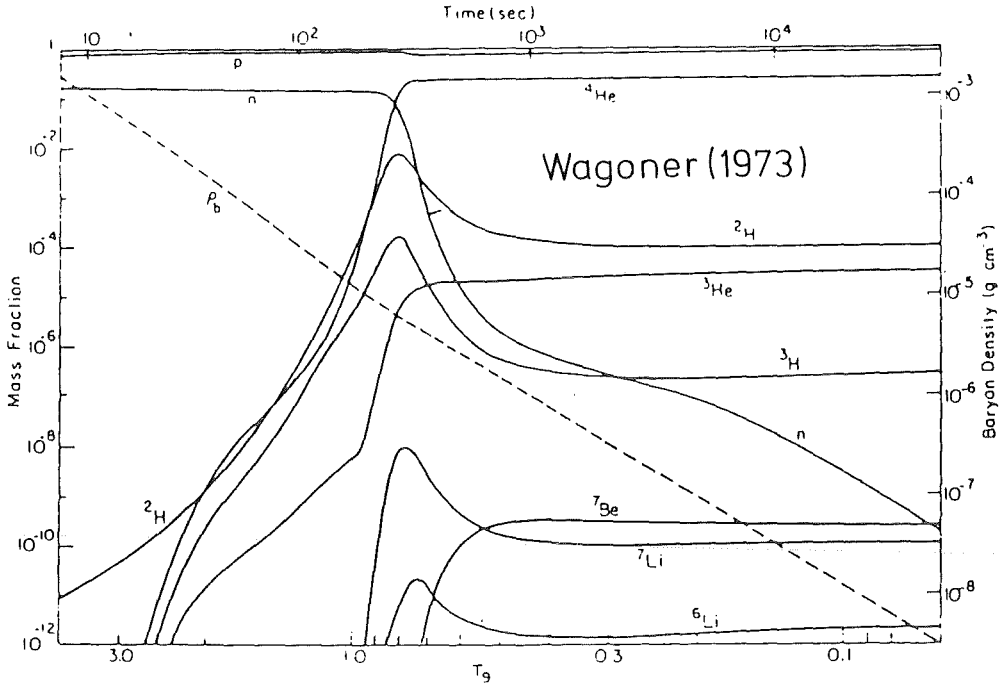

Fig. 5.1 Evolution of the nuclear abundances and baryon density ρ_b during the expansion of the "standard" big-bang (From Ref. 8)

The nucleosynthesis starts at temperatures near 10^9 K ($\hat{=}$ 0.1 MeV) as indicated by Fig. 5.1. The nuclear reaction network, typically involving nuclei $A \leq 12$ (Fig. 5.2) is solved on grounds of a thermodynamical history. The rates are relatively well known for $A \leq 7$ with the exception of the $D(\alpha,\gamma)^6Li$ capture rate. In the framework of the standard big bang model[7] (Friedman- Robertson- Walker - cosmology) the nucleosynthetic yields depend only on one parameter: the baryon density parameter or, equivalently, the *present average universal density of baryons* ρ_B (which scales with $1/T^3$) at T = 2.8 K. This dependence (Fig. 5.3) shows that practically only D, ^{3,4}He and ^{7}Li (those elements which are not made in cosmic rays) are produced in significant quantities. The standard big bang model rests in a large part, on the success in accounting for the observed abundances of the light elements at a *concordant* value of the universal baryon density. The existence (within the uncertainties of the abundances) of such a concordant density provides a consistancy

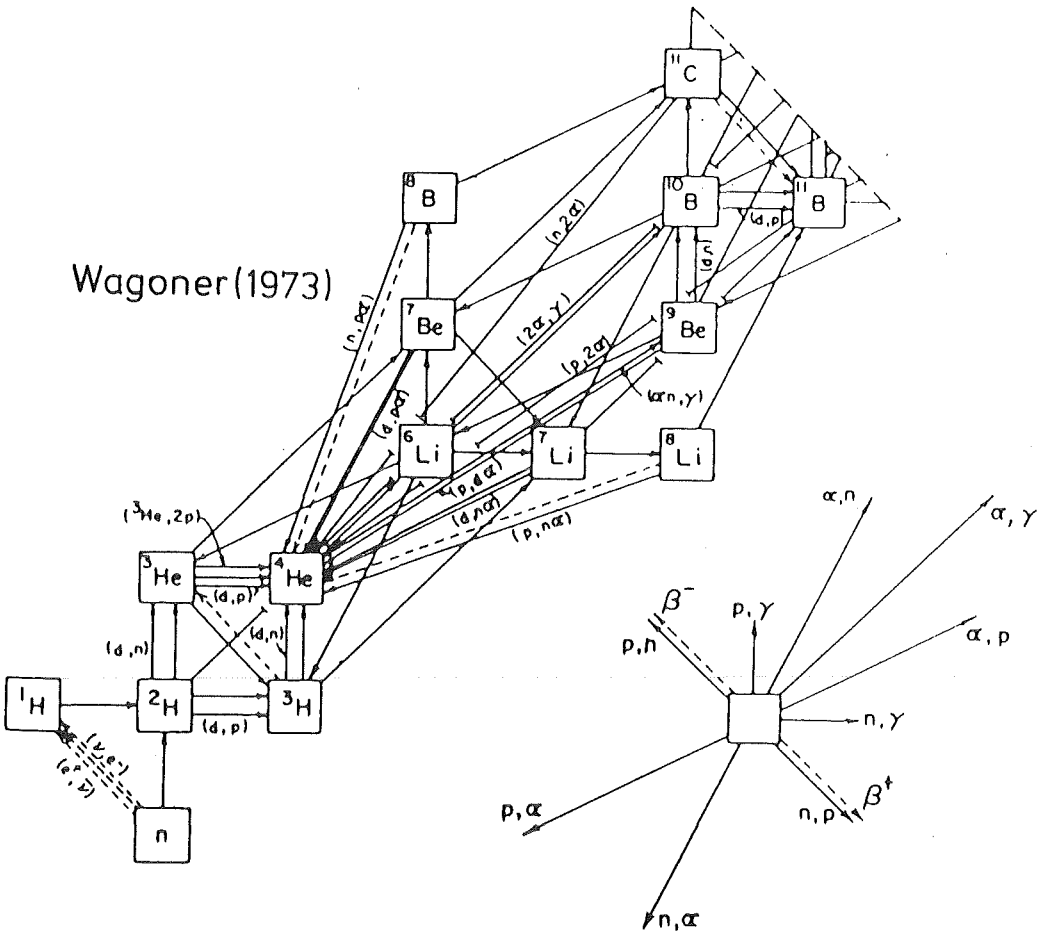

Big bang reaction net work for $A < 12$. All reactions indicated by arrows were included in the calculations of Wagoner (1973). (Adapted from Wagoner 1973.)

Fig. 5.2 The reaction net work for the big bang nucleosynthesis of light elements with A<12 (From Ref. 8)

check of the model. The value itself (otherwise hardly to infer) is of great importance for the cosmological models in view of the questions whether the universe is open and will continue to expand forever, or whether the universe is closed and will eventually collapse again. A detailed understanding of the primordial nucleosynthesis proves to be a powerful probe of the early universe.

It seems that at most few percent of the universal ^{6}Li abundance originates from the big bang nucleosynthesis. However, the calculation of the relevant reaction rate is based on a theoretical extrapolation of the D(α,γ)^{6}Li cross section to energies $E_{\alpha d} \leq 0.1$ MeV. (Fig. 5.4). Experimentally, the cross sections has been investigated only at energies $E_{\alpha d} \geq 1$ MeV, and the data have been analysed on the basis of a capture model[9]. At $E_{\alpha d} = 0.71$ MeV, there is a L = 2 resonance corresponding to the first excited

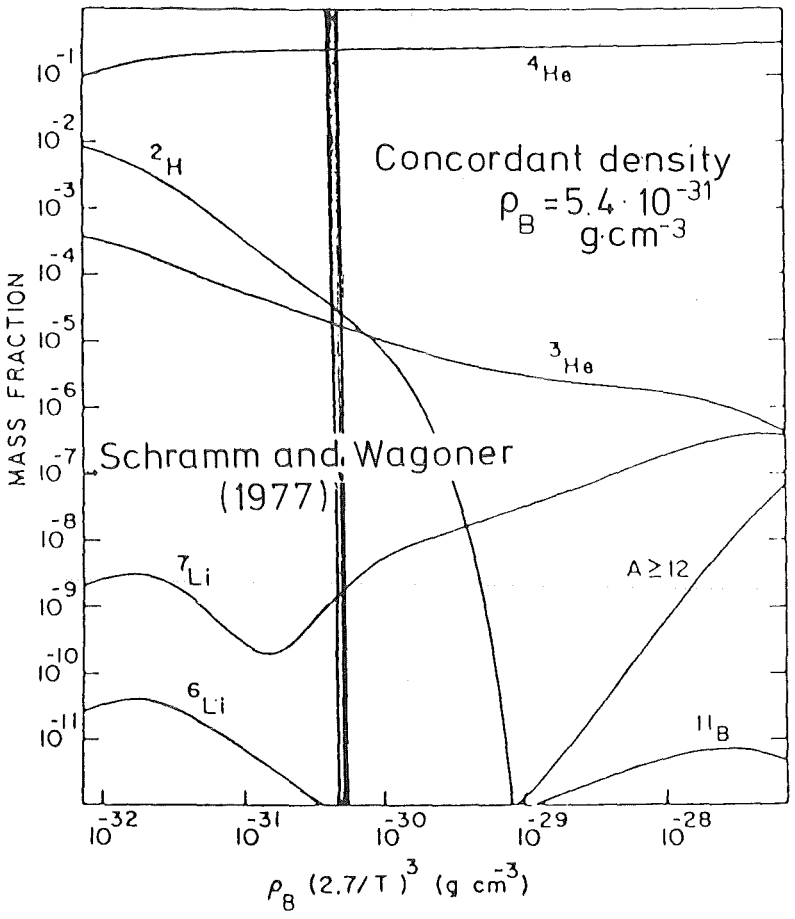

Fig. 5.3 Light element abundances produced in a standard big bang expansion and depending on the *present* value of the baryon density ρ_B. The concordant density inferred from the observed abundances is indicated (Adapted from Ref. 8).

state at $E_{3_1^+}$ = 2.185 MeV in ^{6}Li. The resonance strength can be deduced from the electromagnetic transition probability B(E2; $1^+ \to 3_1^+$) as experimentally determined by the inelastic scattering cross section, ^{6}Li(e,e')^{6}Li e.g.

The resonance cross section is described by a Breit-Wigner-form

$$\sigma(E) = \frac{\pi}{k^2}\,\omega\,\frac{\Gamma_{\alpha d}\,\Gamma_\gamma}{(E_{\alpha d}-E_r)^2+\Gamma^2/4} \qquad (\Gamma = \Gamma_{\alpha d}+\Gamma_\gamma)$$

with $\omega = (2J+1)/[(2j_1+1)(2j_2+1)]$. In the actual case of Γ_γ = $4.4 \cdot 10^{-4}$ eV (Ref.52) << $\Gamma_{\alpha d}$ = 26 keV (Ref.53) $\approx \Gamma$ the peak cross section is given by

$$\sigma_P(E_r) = \frac{4\pi}{k_r^2}\,\omega\,\frac{\Gamma_\gamma}{\Gamma} = \frac{4\pi}{k_r^2}\,\frac{7}{3}\,\frac{\Gamma_\gamma}{\Gamma_{\alpha d}} \approx 107 \text{ nb}$$

(k_r^2 = 0.046 fm^{-2})

ASPECTS OF THE ^{6}Li CASE

(1) Test of the method and the concept

(2) Test of the theory for quadrupole transitions

(3) ^{6}Li production in BIG BANG

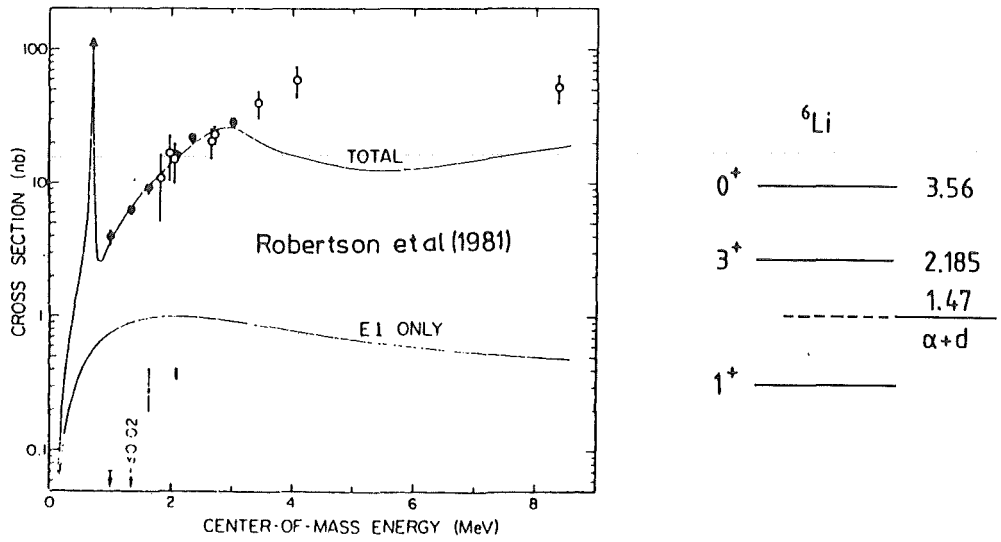

FIG. 1. Cross section for the reaction ^{2}H(α, γ)^{6}Li. Open circles, MSU data; closed circles, CRNL data; triangles, ^{6}Li(e,e'd) (Ref. 7); crosses, CRNL data for E1 component. The curves are a direct-capture calculation.

Fig. 5.4 Cross section for the D(α,γ)^{6}Li capture reaction[9]

When the experimental energy resolution integrates over a window $\Delta >> \Gamma$, the yield is determined by

$$S_r = \int_{E_r-\Delta}^{E_r+\Delta} dE\sigma(E) = \omega\frac{\pi^2}{k^2}\frac{\Gamma_\gamma}{2} = 1.1\cdot10^{-6}\ \text{mb}\cdot\text{MeV}$$

Focusing our experimental efforts to the ^{6}Li case, we have started a series of studies to explore the feasibility of the break-up approach. The experiments are performed at the 156 MeV ^{6}Li beam of the Karlsruhe Isochronous cyclotron using the magnetic spectrometer "Little John"[48] which is especially designed

for the observation at extreme forward emission angles of the ejectiles.

First, the inclusive measurements of the break-up yields have been extended to emission angles smaller than 5°, where Coulomb effects are expected to be dominating. The main experimental difficulties arise from the elastic scattering of ^{6}Li, especially as beam-velocity deuterons and α-particles are focussed onto the same position of the focal plane detector, due to the same magnetic stiffness. Fig. 5.5 shows the energy-integrated inclusive cross sections of the α-particle and deuteron component from collisions of 156 MeV ^{6}Li with ^{208}Pb.

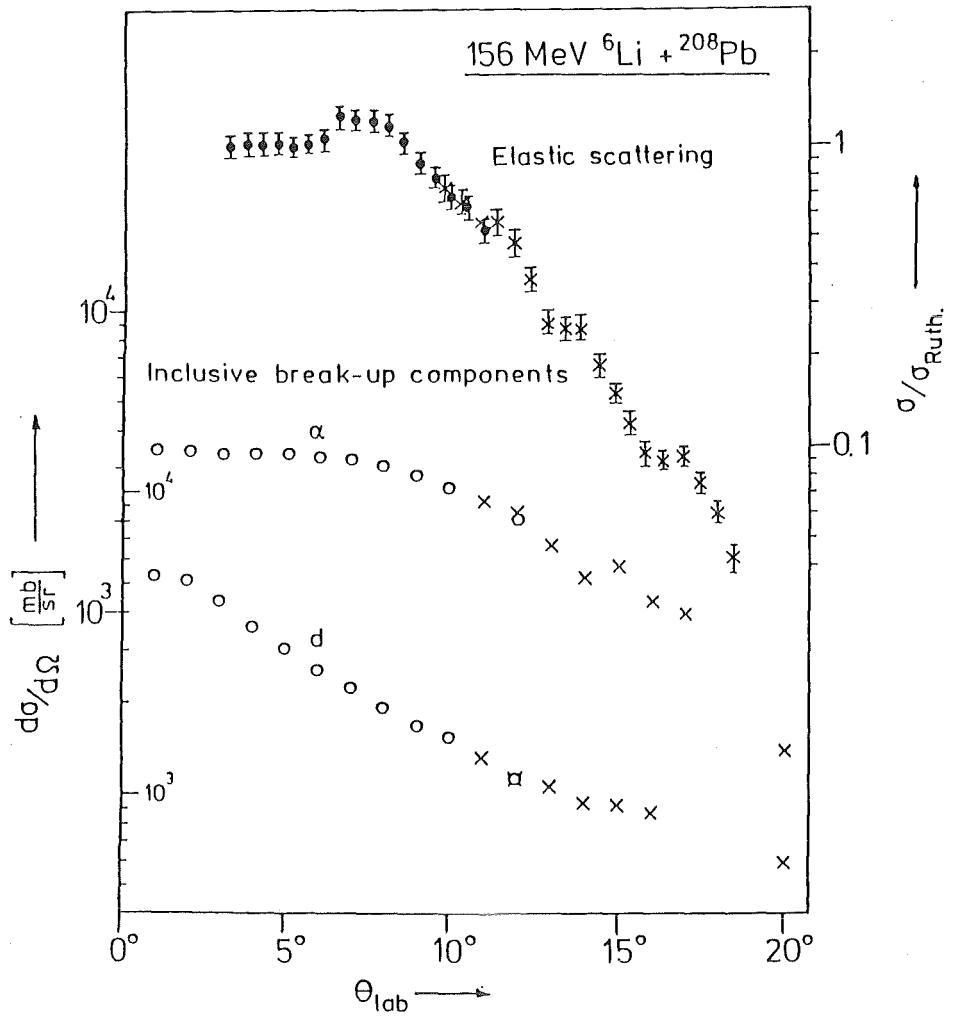

Fig. 5.5 Elastic scattering and inclusive break-up components from 156 MeV ^{6}Li collisions with ^{208}Pb

In order to isolate the elastic component of the break-up bump, i.e. the mode of a correlated emission of deuterons and α-particles leaving the "catalyst" for break-up, the target nucleus, in the ground-state, we have to perform correlation measurements and take advantage of the three-body kinematics described above. Fig. 5.6 shows a first result which corresponds to the kinematic situation of Fig. 4.2. The two peaks of the cross section projected onto the E_α-axis represent the sequential break-up mode via the first excited state of ^{6}Li. Due to unsufficient energy resolution of the solid-state-detector used as second detector, there is some deficiency; the inelastic break-up mode with excitation of the 3^-_1-state in ^{208}Pb is not well separated.

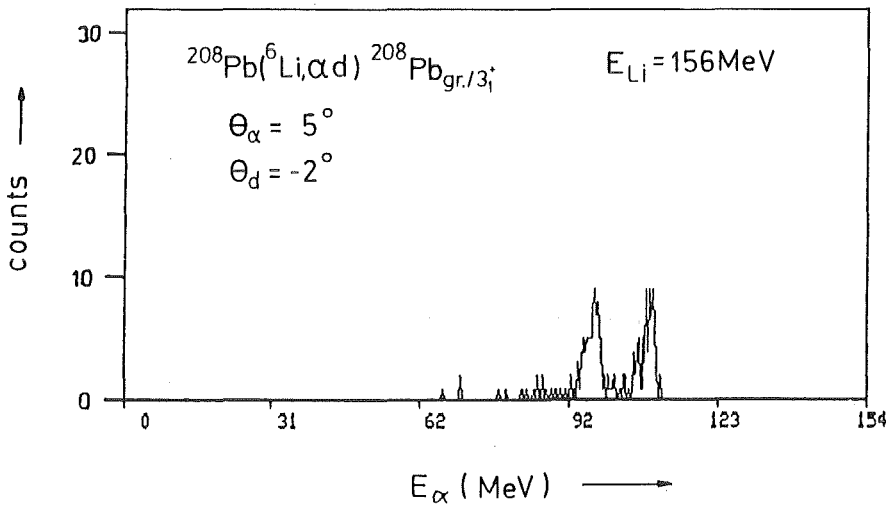

Fig. 5.6 Experimental α-d coincidence spectra at very forward angles from collisions of 156 MeV ^{6}Li-ions with ^{208}Pb.

In any case the result of this test demonstrates that experiments are feasible under this conditions. What we should expect, is displayed in a Monte-Carlo-simulation (Fig. 5.7).

Our interest is directed to the direct (nonresonant) Coulomb break-up of ^{6}Li, not yet discovered up to now and represented by cross-section in regions of the kinematic loci away from reso-

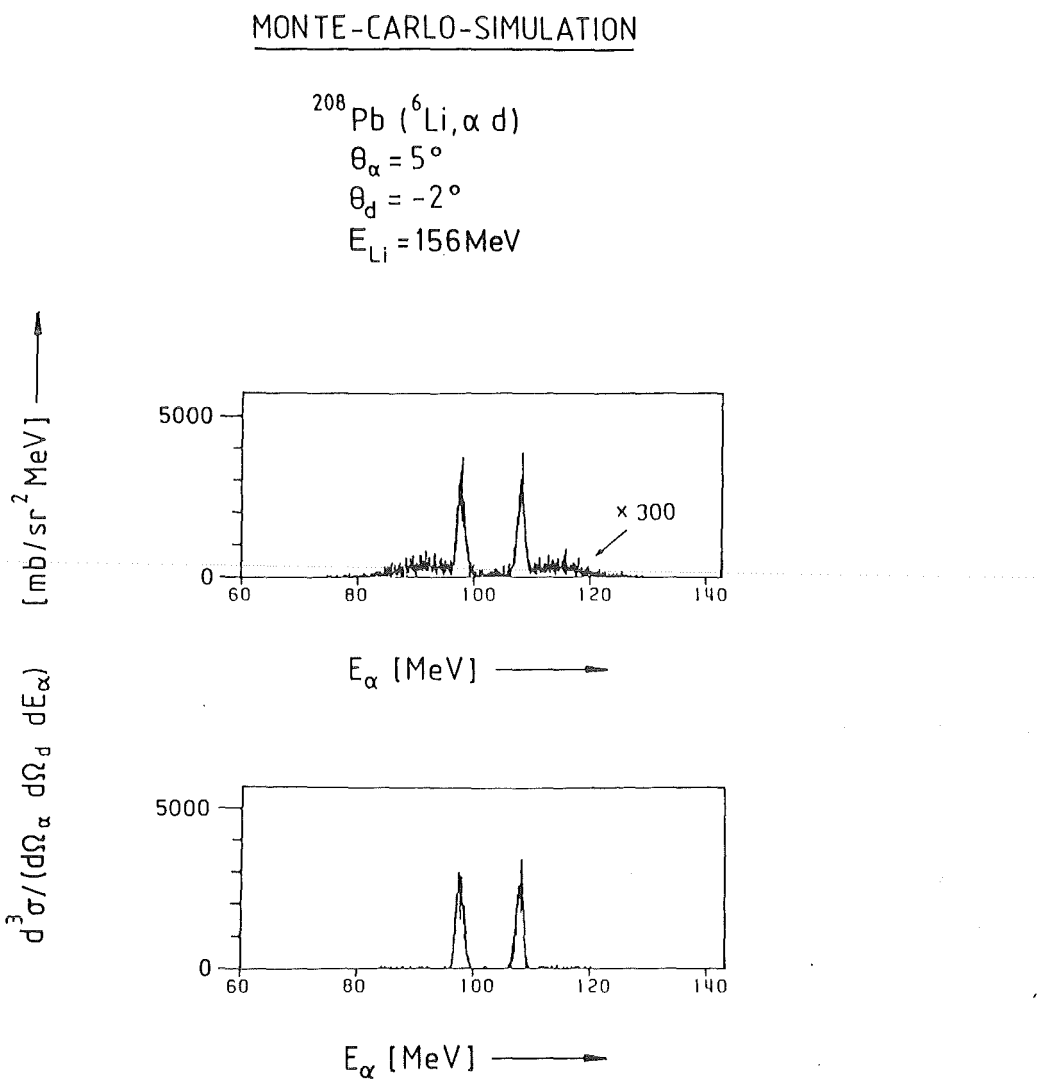

Fig. 5.7 Monte-Carlo-simulation of coincidence (α-d) coincidence spectra

nance peaks from sequential processes. With a narrower angular spacing of the detectors the region of very low relative energies can be considerably stretched (Fig. 5.8)

The upper part of Fig. 5.7 shows (with an enlarged scale) a prediction based on a recent alternative theoretical consideration[12] of the nonresonant Coulomb break-up by a DWBA approach in the Rybicki-Austern[35] formulation of the break-up theory. The Coulomb interaction and the special case L = 2, due to some simplifications the cross section can be (approximately) given by

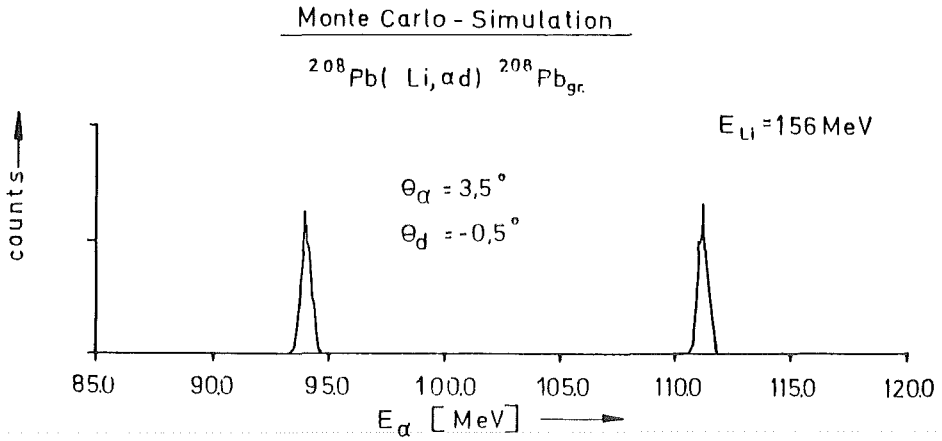

Fig. 5.8 Monte-Carlo-simulation of the coincidence spectra in a very narrow angular geometry

a closed expression in terms of the electromagnetic transition probability $B(E2, E_{\alpha d})$ from the ^{6}Li ground-state into the α-d continuum (Fig. 5.9). With a reasonable estimate of the $B(E2, E_{\alpha d})$ distribution, which can be inferred from the $D(\alpha,\gamma)^6$Li capture cross section (Fig. 5.4), the triple-differential cross section for the Coulomb break-up of ^{6}Li with ^{208}Pb is given in Fig. 5.10.

It is interesting to note that these features resemble very much results of Coulomb break-up of ^{7}Li, studied by Shotter et al. at E_{Li} = 70 MeV. As obvious from Fig. 5.11 (taken from Ref. 24) a direct component become more intense towards forward angles, and our current attempts aim at the observation of the direct (nonresonant) break-up of ^{6}Li, then using the inferred matrix elements for the calculation of the radiative capture cross section.

DWBA APPROACH

OF PROJECTILE BREAK UP

Rybicki and Austern:

$$T_{fi} = \langle \chi^{(-)}_{\vec{Q}_f}(\vec{R})\,\phi^{(-)}_k(\vec{r}) \,|\, V_{res}(\vec{R},\vec{r}) \,|\, \chi^{(+)}_{Q_i}(\vec{R})\,\phi_a(\vec{r}) \rangle$$

$$V_{res} = z_\Lambda e^2 \left(\frac{z_b}{r_{b\Lambda}} + \frac{z_x}{r_{x\Lambda}} - \frac{z_a}{R}\right)$$

$$= 4\pi z_\Lambda e^2 \sum_{L,M\geq 1} \left(z_b \left(-\frac{m_x}{m_a}\right)^L + z_x \left(\frac{m_b}{m_u}\right)^L \right) \frac{r^L}{R^{L+1}}$$

$$* \frac{1}{2L+1} \cdot Y^*_{LM}(\hat{R}) \cdot Y_{LM}(\hat{r})$$

Quadrupole case L = 2

$$^6Li \rightarrow \alpha + d$$

$$\frac{d^3\sigma}{d\Omega_\alpha\, d\Omega_d\, dE_\alpha} = \frac{(4\pi)^4}{90\,\hbar} \frac{Z_A^2 e^2}{(2I_f+1)} \sqrt{\frac{m_{Li}}{E^{Lab}_{Li}}}\; C^2(\eta, E_{\alpha d}) *$$

$$B(E2;\, E_\alpha(E_{\alpha d}))$$

Fig. 5.9 Quasi-sequential DWBA approach [12] of Coulomb break-up of ^{6}Li projectiles.

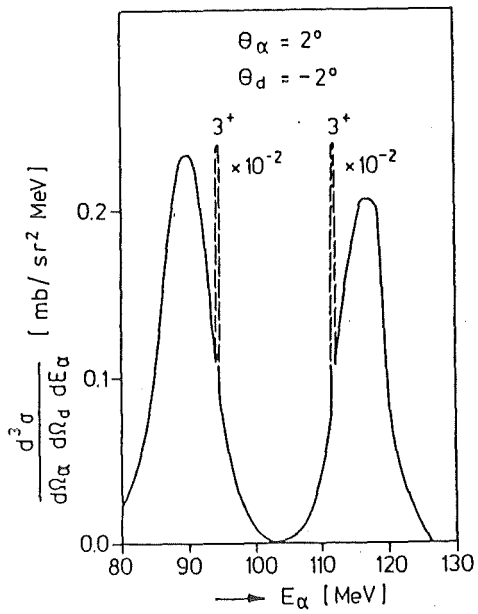

Fig. 5.10
Resonant and nonresonant excitation of the α+d continuum in ^{6}Li by projectile break-up in the Coulomb field of ^{208}Pb at E_{Li} = 156 MeV as calculated on the basis of a DWBA approach[12].

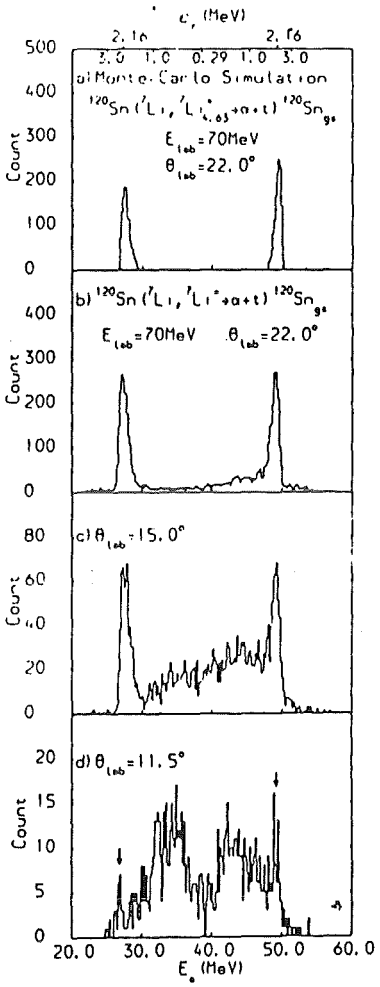

(a) α-energy spectrum for sequential breakup of ^{7}Li using a Monte Carlo simulation. (b)–(d) Experimental α-energy spectra of the reaction ^{120}Sn(^{7}Li, ^{7}Li* → α + t)^{120}Sn$_{g.s.}$ at 22°, 15°, and 11.5°.

Fig. 5.11
Resonant and nonresonant Coulomb break-up of ^{7}Li at E_{Li} = 70 MeV (Ref. 24).

6. CONCLUSIONS

"Quantum valerent inter homines litterae,
Dixi superius: quantus nunc illis honos
A superis sit tributus tradam memoriae"

Phaedrus, Liber Fabularum

The proposed approach for studies of the interaction of nuclear particles at small relative energies requires experiments at extreme forward angles, in a region where $\sigma_{elastic}/\sigma_R = 1$. The elastic scattering cross section provides, in fact, a calibration of the break-up cross sections. The values of the estimated coincidence cross sections are rather small, but appear to be measurable by present days' experimental techniques. The kinematic situation with three outgoing particles provides particular advantages for studies of the excitation function i.e. the variation with relative energy of the emerging fragments, and of the angular distribution in the rest frame of the fragments subsystems. Investigations of the latter aspect, however require a quite good angular resolution. The cross sections can be interpreted in terms of electromagnetic interaction matrix elements which just determine the radiative capture cross section. There are a number of problems which have to be investigated in more detail, experimentally mainly arising from the dominance of elastic Coulomb scattering. The theory has to be refined with respect to orbital dispersion and Coulomb distortion effects[54].

Very interesting and improved experimental possibilities would be provided by a dedicated set up at a synchrotron-cooler ring (see Ref. 49) with suitable magnetic spectrometers (such as the proposal of Ref. 50), enabling particle coincidence studies at very forward emission directions. The use of a storage ring seems to be indispensable when working with radioactive beams like with ^{7}Be. Even, if the acceleration and preparation of such a beam would be successful in a conventional approach, the contamination problems arising from the accumulation of the radioactivity ($T_{1/2}[^7\text{Be}] = 53.3$ d) impose serious limits. On the

Table 6.1 Radiative capture reactions of interest for light element nucleosynthesis

$^{3}He(\alpha,\gamma)^{7}Be$	(53.3 d)	Solar neutrino problem
$^{7}Be(p,\gamma)^{8}B$	(770 ms)	^{3}He abundancy
$^{7}Be(\alpha,\gamma)^{11}C$	(20.4 m)	
$^{4}He(d,\gamma)^{6}Li$	(stab.)	Primordial nucleosynthesis
$^{6}Li(p,\gamma)^{7}Be$	(53.3 d)	of Li Be B - isotopes
$^{6}Li(\alpha,\gamma)^{10}B$	(stab.)	
$^{4}He(^{3}He,\gamma)^{7}Li$	(stab.)	
$^{7}Li(\alpha,\gamma)^{11}B$	(stab.)	
$^{11}B(p,\gamma)^{12}C$	(stab.)	
$^{9}Be(p,\gamma)^{10}B$	(stab.)	
$^{10}B(p,\gamma)^{11}C$	(20.4 m)	
$^{12}C(p,\gamma)^{13}N$	(10 m)	CNO - cycles
$^{16}O(p,\gamma)^{17}F$	(65s)	
$^{13}N(p,\gamma)^{14}O$	(70.6s)	
$^{20}Ne(p,\gamma)^{21}Na$	(22.5s)	
$^{15}O(\alpha,\gamma)^{19}Ne$	(17.2s)	RP - Process
$^{12}C(\alpha,\gamma)^{16}O$	(stab.)	Helium-burning
$^{16}O(\alpha,\gamma)^{20}Ne$	(stab.)	
$^{14}N(\alpha,\gamma)^{18}F$	(109.7 m)	

other side, in a storage ring, even a current of 10 mA corresponds to a sufficiently small number of stored radioactive particles. A Hg vapour jet target[51] e.g. may serve as reaction target for the Coulomb break-up measurements.

Table 6.1 compiles some examples of radiative capture reactions of light nuclei which may be studied by the inverse process (the dissociation), some requiring the availibility of beams of radioactive ions. The reactions are of interest at various astrophysical sites and at different temperatures, some of them only for explosive burning processes at higher temperatures (i.e. for higher relative energies of the interacting charged particles).

Though each case will require specific considerations concerning the experimental feasibility, such a list may indicate the wide field of interesting problems which can be attacked with the method.

I would like to thank Dr. G. Baur, Dr. C.A. Bertulani and Dr. D.K. Srivastava for a fruitful collaboration in the theoretical foundation of the method, and Dr. H.J. Gils, DP H. Jelitto and Prof. Dr. G. Schatz for many clarifying discussions and contributions to experimental aspects of Coulomb dissociation studies. Valuable and encouraging comments of Prof. Dr. H.A. Weidenmüller and Dr.I.M. Brâncuș are gratefully acknowledged.

7. REFERENCES

1. W.A. Fowler, Rev. Mod. Phys. 56 (1984) 149
2. C. Rolfs and H.P. Trautvetter, Ann. Rev. Nucl. Sci. 28 (1978) 115
3. T. Kajino and A. Arima, Phys. Rev. Lett. 52 (1984) 739
4. J.L. Osborne, C.A. Barnes, R.W. Kavanagh, R.M. Kremer, G.J. Mathews, J.L. Zyskind, P.D. Parker, and A.J. Howard, Phys. Rev. Lett. 48 (1982) 1664 - Nucl. Phys. A419 (1984) 115
5. K. Nagatani, M.R. Dwarakanath, and D. Ashery, Nucl. Phys. A 128 (1969) 325
6. K.U. Kettner, H.W. Becker, L. Buchmann, J. Görres, H. Krähwinkel, C. Rolfs, P. Schmalbrock, H.P. Trautvetter, and A. Vlieks, Z. Phys. A 308 (1982) 73
   K. Langanke and S.E. Koonin, Nucl. Phys. A 439 (1985) 384
   Q.K.K. Liu, H. Kanada, and V.C. Tang, Phys. Rev. C 33 (1986) 1561
7. S.M. Austin, Prog. Part. Nucl. Phys. 7 (1981) 1
8. R.V. Wagoner, Astrophys. J. 179 (1973) 343; D.N. Schramm and R.V. Wagoner, Ann. Rev. Nucl. Sci. 27 (1977) 37
9. R.G.H. Robertson, P. Dyer, R.A. Warner, R.C. Melin, T.J. Bowles, A.B. McDonald, G.C. Ball, W.G. Davies, and E.D. Earle, Phys. Rev. Lett. 47 (1981) 1867
10. D.N. Schramm, Nature 317 (1985) 386
11. H. Rebel, Workshop "Nuclear Reaction Cross Sections of Astrophysical Interest" unpublished report, Kernforschungszentrum Karlsruhe, February 1985.
12. D.K. Srivastava and H. Rebel, Journ.Phys.G: Nucl.Phys. 12 (1986) 717
13. G. Baur, C.A. Bertulani and H. Rebel, Nucl. Phys. A 458 (1986) 188; KfK-Report 4037 (Jan. 1986); Contr. Internat. Symposium on Weak and Electromagnetic Interactions in Nuclei, 1-5 July 1986, Heidelberg (Germany)
    G. Baur, Lecture presented at the 1985 Varna International Summer School on Nuclear Physics, Sept. 22 - Oct. 1, 1985

14. B. Neumann, H. Rebel, J. Buschmann, H.J. Gils, H. Klewe-Nebenius and S. Zagromski, Z. Phys. A 296 (1980) 113

15. B. Neumann, H. Rebel, H.J. Gils, R. Planeta, J. Buschmann, H. Klewe-Nebenius, S. Zagromski, R. Shyam and H. Machner, Nucl. Phys. A 382 (1982) 296
B. Neumann, J. Buschmann, H. Klewe-Nebenius, H. Rebel and H.J. Gils, Nucl. Phys. A 329 (1979) 150

16. W. von Oertzen, private communication

17. G. Baur, F. Rösel, D. Trautmann and R. Shyam, Phys. Rep. C 111 (1984) 334; G. Baur and D. Trautmann, Phys. Rep. C 25 (1976) 291

18. R.J. de Meijer, R. Kamermans, Rev. Mod. Physics 57 (1985) 147

19. C.M. Castastaneda, H.A. Smith Jr., P.P. Singh and H. Karwowski, Phys. Rev. C 21 (1980) 179

20. A.C. Shotter, in Proc. 4th Int. Conference on Clustering Aspects of Nuclear Structure and Nuclear Reactions, Chester, U.K. 23-27 July, 1984; D. Reidel Publ. Company, p. 199 ff

21. H. Utsunomija, Phys. Rev. C 30 (1984) 1748

22. H. Utsunomija, S. Kubono, M.M. Tanaka, M. Sugitani and K. Morita, T. Nomura, Y. Hamaijama, Phys. Rev. C 28 (1984) 1975

23. A.C. Shotter, Phys. Lett. 46 (1981) 12

24. A.C. Shotter, V. Rapp, T. Davinson, D. Branford, N.E. Sanderson and M.A. Nagarajan, Phys. Rev. Lett 53 (1984) 1539

25. J.Unternährer, J. Lang and R. Müller, Phys. Rev. Lett. 40 (1978) 1013

26. A. Pop, M. Cenja, M. Duma, R. Dumitrescu, A. Isbasescu and M.T. Magda, IPNE-preprint NP-32 (1986)

27. J.F. Mateja, J. German, A.D. Frawley, Phys. Rev. C 28 (1983) 1579

28. S.L. Tabor, L.C. Denis, K. Abdo, Phys. Rev. C 24 (1981) 2552

29. S.L. Tabor, L.C. Denis, K.W. Kemper, J.D. Fox, K. Abdo, G. Neuschafer, D.G. Kovar, H. Ernst, Phys. Rev. C 24 (1981) 960

30. W.D.M. Rae, A.J. Cole, B.G. Harvey and R.G. Stokstad, Phys. Rev. C 30 (1984) 158

31. A. Pop, M. Cenja, M. Duma, R. Dumitrescu, A. Isbasescu, M.T. Magda, Revue Roumaine de Phys. 29 (1984) 87

32. M.T. Magda, A. Pop, A. Sandulescu, J. Phys. G 11 (1985) L75

33. R. Serber, Phys. Rev. 72 (1947) 1008

34. G. Baur, Z. Phys. A 277 (1976) 147

35. F. Rybicki and N. Austern, Phys. Rev. C 6 (1971) 1525

36. D.K. Srivastava and H. Rebel, Phys. Rev. C 33 (1986) 1221

37. E.M.L. Aarts, R.A.R.L. Malfliet, R.J. de Meijer and S.Y. van der Werf, Nucl. Phys. A 425 (1984) 23
E.M.L. Aarts, R.A.R.L. Malfliet, R.J. de Meijer, S.Y. van der Werf, G. Baur, R. Shyam, F. Rösel and D. Trautmann, Nucl. Phys. A 439 (1985) 45

38. D.K. Srivastava, Lectures presented at the XVIIth Internat. Summer School on Nuclear Physics, Mikolajki, Poland, Sept. 1985 - KfK-Report 4007

39. R. Płaneta, H. Klewe-Nebenius, J. Buschmann, H.J. Gils, H. Rebel, S. Zagromski, T. Kozik, L. Freindl and K. Grotowski, Nucl. Phys. A 448 (1986) 110

40. Conf. on Correlations of Particles Emitted in Nuclear Reactions, Rev. Mod. Phys. 37 (1965) 327

41. G. Baur, Phys. Lett. B (in press)
Lecture presented at the 1985 Varna Internat. School on Nucl. Physics, Sept. 22 - Oct. 1, 1985, Varna, Bulgaria

42. K. Alder and A. Winther, Electromagnetic Excitation (North-Holland, Amsterdam, 1975)
K. Alder and A. Winther, Coulomb Excitation (Academic Press, New York 1966)

43. C.A. Bertulani and G. Baur, Nucl. Phys. A 442 (1985) 739;
A. Goldberg, Nucl. Phys. A 420 (1984) 636

44. G.G. Ohlsen, Nucl. Instr. Meth. 37 (1970) 240

45. H. Fuchs, Nucl. Instr. Meth. 200 (1982) 361

46. H. Reeves, W.A. Fowler and F. Hoyle, Nature 226 (1970) 727

47. J. Yang, M.S. Turner, G. Steigman, D.N. Schramm and K.A. Oleve, Astrophys. J. 281 (1981) 493

48. H.J. Gils, KfK-Report 2972 (1980)
H.J. Gils, J. Buschmann, S. Zagromski, H. Rebel, J. Krisch, M. Heinz, Internal Reports Kernforschungszentrum Karlsruhe

49. COSY, Proposal for a cooler-synchotron as a facility for nuclear and intermediate energy physics at the KFA Jülich, Jülich 1985; KFA Jülich - Jül-Spez-242 Februar 1984 ISSB 0343 - 7639; Workshop on Physics with Heavy Ion Cooler Rings, Max-Planck-Institut für Kernphysik, Heidelberg 1981

50. J.W. Sunier, K.D. Bol, M.R. Clover, R.M. De Vries, N.J. Di Giacomo, J.S. Kapustinsky, P.L. McGaughey and W.E. Sondheim, Nucl. Instr. and Meth. A 241 (1985) 139

51. G. Montagnoli, H. Morinaga, U. Ratzinger and P. Rostek, Jahresbericht 1984 des Beschleunigerlaboratoriums der Universität und Technischen Universität München, contr. 4.2.3. p. 109

52. F. Eigenbrod, Z. Phys. 238 (1969) 337

53. F. Ajzenberg-Selove and T. Lauritsen, Nucl. Phys. A 214 (1973) p. 33

54. J. Pochodzalla, C.K. Gelbke, C.B. Chitwood, D.J. Fields, W.G. Lynch, M.B. Tsang and W.A. Friedman, Phys. Lett. 175 B (1986) 275